

Large scale structure analysis with galaxy redshift surveys II

Florian Beutler

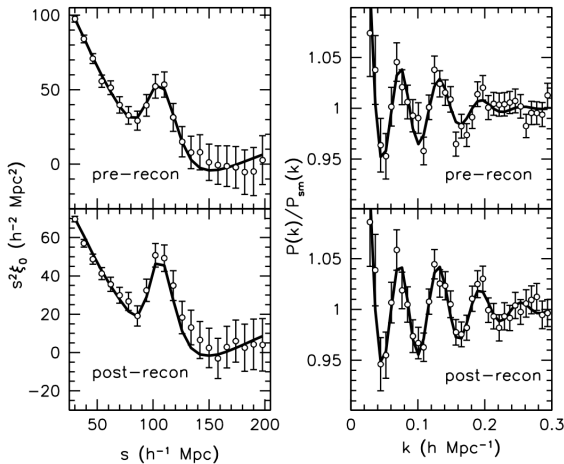
June, 2015



Lawrence Berkeley National Lab

Recap what we learned about BAO

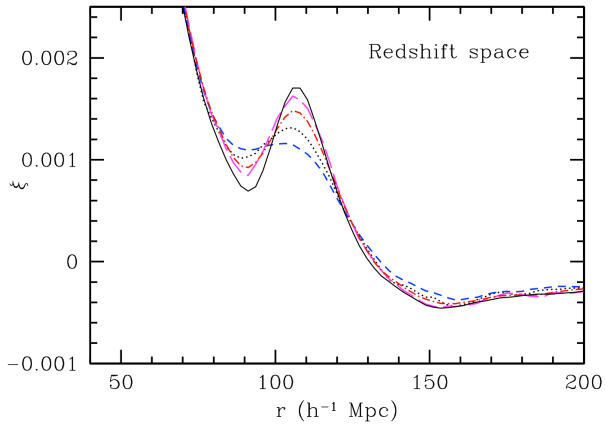
1. BAO is a localized feature in the correlation function and an oscillating feature in the power spectrum.



Anderson et al 2014

Recap what we learned about BAO

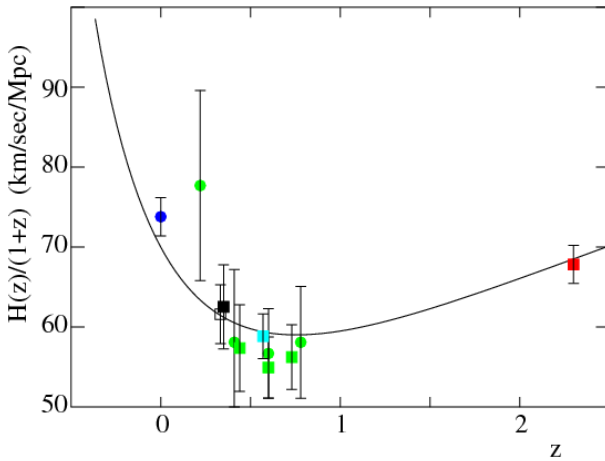
2. Density field reconstruction can increase the signal-to-noise of BAO measurements by up to a factor of 2... depending on redshift.



Eisenstein et al. (2007), Padmanabhan et al. (2012)

Recap what we learned about BAO

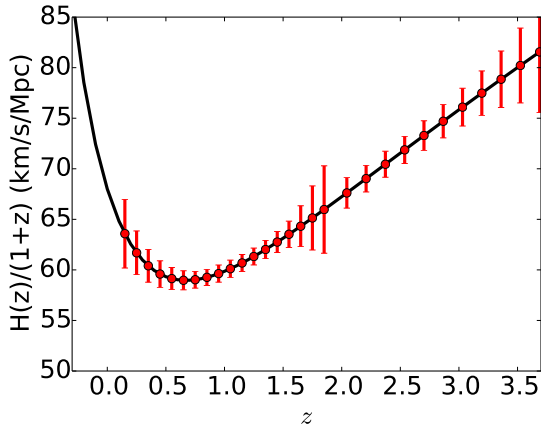
3. Using the Lyman- α forest we can make BAO distance measurements at redshift 2.5, much further than current supernovae distance measurements.



Busca et al. (2013)

Recap what we learned about BAO

4. Future galaxy survey projects like DESI and Euclid will map out the expansion history with sub-% level precision up to redshift 3.5.



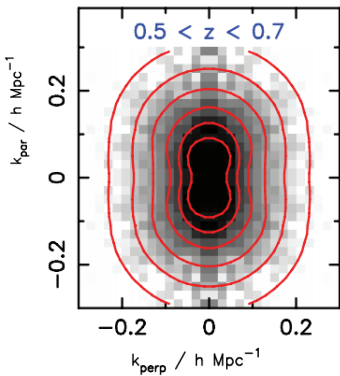
credit: Patrick McDonald

Outline of the talk

- What are Redshift-space distortions?
- Galaxy survey specific difficulties beyond what we discussed already.
- Modeling redshift-space distortions.
- Current results
- Future outlook
- Other observables: Neutrino mass and non-Gaussianity

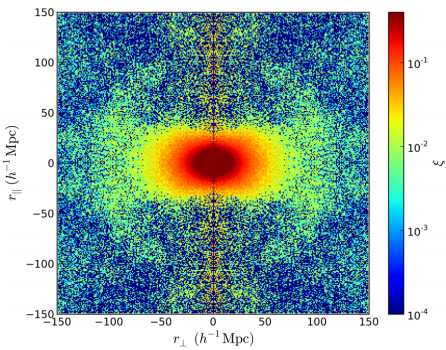
Anisotropy in the observed $\xi(r, \mu)$ and $P(k, \mu)$

2D power spectrum



Blake et al. (2011)

2D correlation function

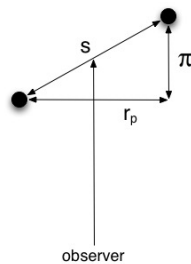


Samushia et al. (2014)

Redshift-space distortions

- The observed two-dimensional ξ/P function is clearly anisotropic, plotted as a function of transverse and line-of-sight (LOS) distances.
- Some of this is caused by the AP effect, but the primary source of this anisotropy is redshift space distortions (RSD).
- The observed spectroscopic redshift is given by

$$z_{\text{spec}} = z_{\text{cosmo}} + \frac{v_p^{\text{LOS}}}{ac}$$



- The second term comes from the peculiar velocity of the galaxy due to inhomogeneities in its local environment

Redshift-space distortions

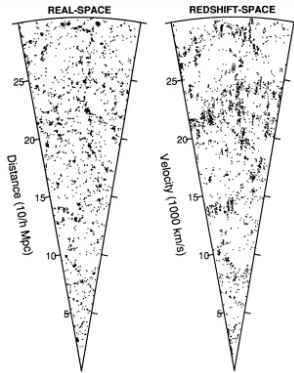
$$z_{\text{spec}} = z_{\text{cosmo}} + \frac{v_p^{\text{LOS}}}{ac}$$

- Since we cannot separate the two terms on an object-by-object basis, we simply infer the radial coordinate of the object assuming $v_p^{\text{LOS}} = 0$ when generating 3D galaxy density maps. This leaves coherent distortions in the galaxy maps, since the galaxy density and velocity fields are correlated.
- Propagating the v_p term we find

$$\chi(z_{\text{spec}}) = \chi(z_{\text{cosmo}}) + \frac{v_p^{\text{LOS}}}{aH}$$

Redshift-space distortions

When distances are inferred from redshifts like this, we call the coordinate system redshift-space (usually labelled with s), in contrast to real-space (labeled with r), which we can't measure (except in a simulation). These distortions can be seen in the galaxy maps.

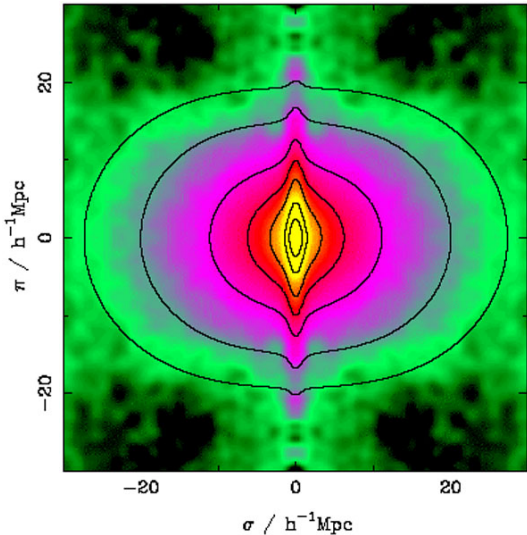


Praton et al. (1997)

The 2014 Shaw prize

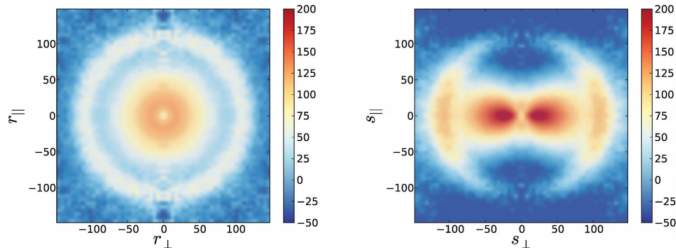


Redshift-space distortions



Peacock et al. (2001)

Redshift-space distortions



- In real-space the 2D correlation function is circular
- Redshift space distortions contribute the additional term $v_p^{\text{LOS}}/(aH)$ in the sense that

$$\chi(z) = \chi_{\text{true}} + \frac{v_p^{\text{LOS}}}{aH}$$

- The peculiar velocity terms follows the linearized continuity eq.

$$\nabla \cdot v_p = -aHf\delta_m$$

- The peculiar velocity term is given by

$$|v_p| \sim \frac{d\sigma_8}{d \ln a} = f\sigma_8$$

where the growth f is given $f \approx \Omega_m^{0.55}$ (e.g. Linder 2005).

- This means that by measuring the anisotropy of clustering, we should be able to measure $d\sigma_8/d \ln a$, the growth rate of cosmic structure.
- RSD and AP are both introducing anisotropy, but they are not degenerate, since they have different scale dependence.
- Dark Energy Task Force 3rd report: RSD is “among the most powerful ways of addressing whether the acceleration is caused by dark energy or modified gravity”

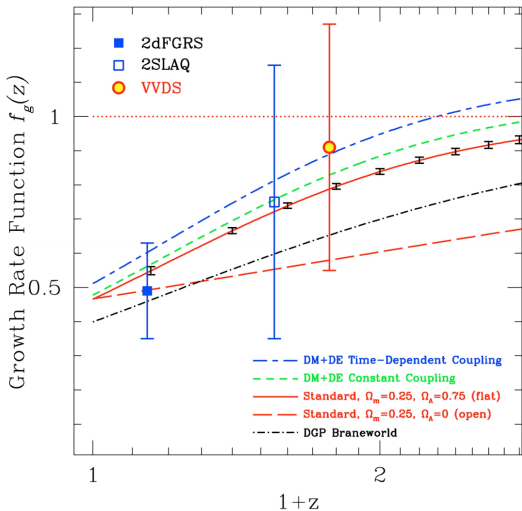
Why measuring RSD?

- In GR, the growth of linear perturbations is scale independent (does not depend on k).
- In GR, the growth of linear perturbations is determined by the cosmic expansion history:

$$\frac{d^2 D}{d \ln a^2} + \left(2 + \frac{d \ln H}{d \ln a} \right) \frac{d D}{d \ln a} = \frac{3}{2} \Omega_m(a) D$$

- Modified gravity, dark sector interactions, massive neutrinos, etc. can potentially break GR predictions.
- This is why we should measure both the expansion and growth history as precisely as possible.
- So the idea is we constrain the background cosmology with CMB and BAO and constrain GR with the growth of structure measurements, which usually need some priors on the background cosmology.

Redshift-space distortions



Guzzo et al. 2008

- We will work in the plane-parallel approximation (LOS is along a single Cartesian axis z rather than spherical coordinates).
- Start with the conservation of tracers:

$$(1 + \delta_g^s) d^3 s = (1 + \delta_g) d^3 r$$

- Compute the Jacobian of the $d^3 r \rightarrow d^3 s$ transformation

$$\frac{d^3 s}{d^3 r} = \left(1 + \frac{v_z}{z}\right)^2 \left(1 + \frac{dv_z}{dz}\right)$$

neglect $v_z/z \ll 1$.

$$1 + \delta_g^s = (1 + \delta_g) \left(1 + \frac{dv_z}{dz} \right)$$

- Assuming v is irrotational we can write the density field in redshift-space as

$$\delta_g^s(k) = \delta_g(k) + \mu^2 \theta(k)$$

with $\theta = -\nabla \cdot v$ ($dv_z/dz = k_z^2/k^2 \theta(k) = \mu^2 \theta(k)$).

- Often people assume that the velocity field comes from linear PT, which allows to relate θ and δ by

$$\theta(k) = \beta \delta_g(k) = f \delta_m(k).$$

- We get a really simple result. Each k -mode remains independent with the same phases as in real space, with amplitude enhanced depending on μ^2 .

- Squaring this result gives the power spectrum in redshift space (Kaiser formula, see Kaiser (1987)):

$$P_g^s(k, \mu) = (b + f\mu^2)^2 P_m^r(k) = b^2(1 + \beta\mu^2)^2 P_m^r(k)$$

- The difficulties of knowing the galaxy bias b destroys (all) information of the amplitude (σ_8), but the angular dependence of the RSD signal can still be used. For that we marginalize over the unknown amplitude ($b\sigma_8$), leaving the observable $f\sigma_8 = \beta b\sigma_8$.

Multipole decomposition

As discussed before, we want to minimize the number of elements in our data vector, so we don't want to use bins in $\xi(s, \mu)$ or $P(k, \mu)$. We use multipole decomposition:

$$P(k, \mu) = \sum_{\ell} P_{\ell}(k) \mathcal{L}_{\ell}(\mu)$$

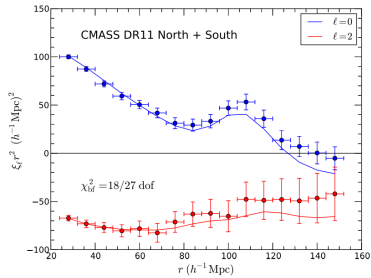
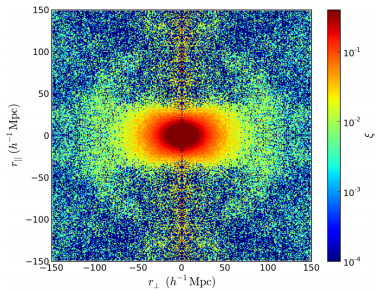
$$\xi(s, \mu) = \sum_{\ell} \xi_{\ell}(s) \mathcal{L}_{\ell}(\mu)$$

And they are simply related by a Henkel transform

$$\xi_{\ell}(s) = i^{\ell} \int \frac{k^2 dk}{2\pi^2} P_{\ell}(k) j_{\ell}(ks)$$

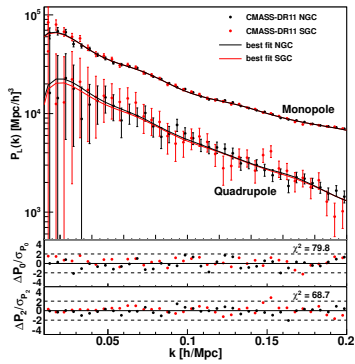
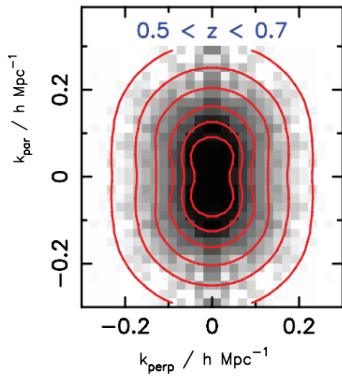
Multipole decomposition

Correlation function multipoles:



Multipole decomposition

Power spectrum multipoles:



- While for BAO we did not have to bother about modeling the power spectrum shape exactly, in the case of RSD we can't ignore the shape.
- The linear model only works on very large scales, but most of the modes are at small scales. Going beyond linear theory might allow us to include smaller scales and could significantly improve cosmological constraints.
- Lots of complicated physical effects the galaxy ξ/P away from its linear theory behavior:
 - non-linear gravitational evolution
 - non-linear biasing between tracers and matter field
 - non-linear redshift space distortions

Modeling the galaxy power spectrum

- We can express the galaxy density fluctuation field, $\delta_g(x)$, in terms of the matter field $\delta_m(x)$ in a Taylor expansion

$$\delta_g(x) = \epsilon + b_1 \delta_m(x) + \frac{1}{2} b_2 \delta_m^2(x) + \frac{1}{6} b_3 \delta_m^3(x) + \dots$$

with the bias coefficients b .

- Now we have to turn this into Fourier-space and determine the different correlation terms... see Saito et al. 2009 appendix C
- The power spectrum can be written as

$$P_g(k) = b_1^2 P_{\text{lin}}(k) + b_1 b_2 P_{b2}(k) + b_2^2 P_{b22}(k) + N$$

with

$$P_{b2}(k) = 2 \int \frac{d^3 q}{(2\pi)^3} P_m^L(q) P_m^L(k-q) F^{(2)}(q, k-q)$$

$$P_{b22}(k) = \frac{1}{2} \int \frac{d^3 q}{(2\pi)^3} P_m^L(q) \left[P_m^L(|k-q|) - P_m^L(q) \right]$$

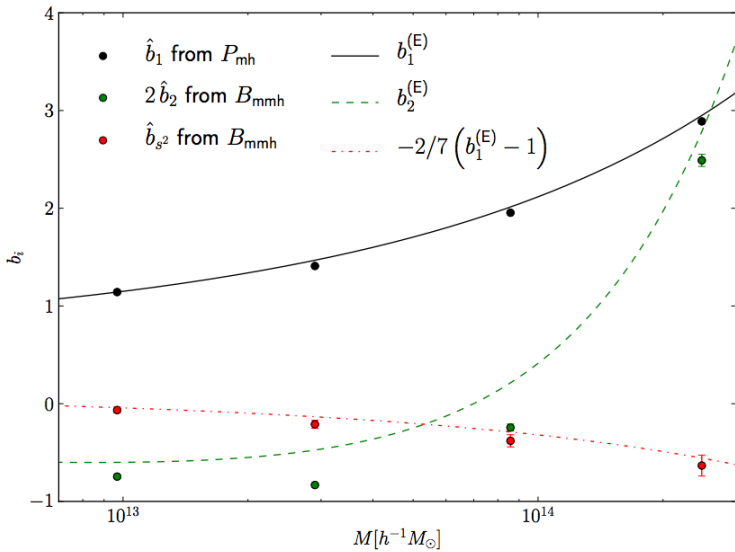
Modeling the galaxy power spectrum

- With the kernel

$$F(k, k') = \frac{5}{7} + \frac{1}{2} \frac{k \cdot k'}{kk'} \left(\frac{k'}{k} + \frac{k}{k'} \right) + \frac{2}{7} \left(\frac{k \cdot k'}{kk'} \right)^2$$

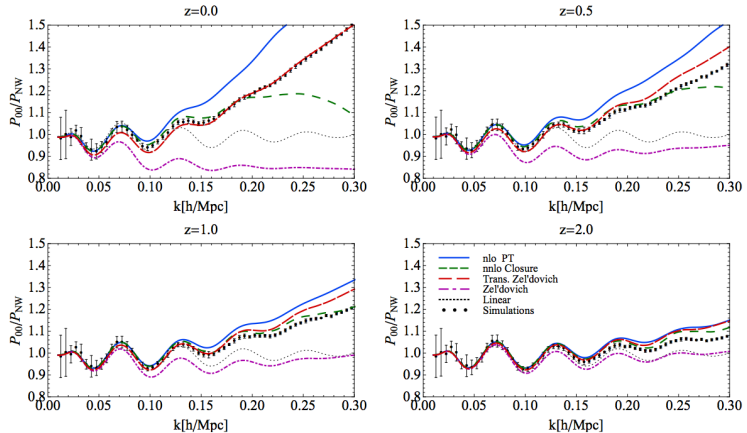
- The terms multiplying b_2 give rise to a scale-dependent bias due to the non-linear clustering.
- In general b_1 , b_2 and N vary with galaxy type. So we can't predict it from theory but need to constrain it from the data.

Galaxy biasing



Baldauf et al. (2012)

perturbation theory



Vlah et al. (2012)

Modeling the galaxy power spectrum

- When we tailor expanded the density field earlier we assumed that the galaxy density field depends only on the local matter density field. But that does not need to be true.

$$\delta_g(x) = \epsilon + b_1\delta_m(x) + \frac{1}{2}b_2\delta_m^2(x) + \frac{1}{6}b_3\delta_m^3(x) + [b_{2,nl} + \dots + b_{3,nl}\dots]$$

$b_{2,nl}$ seems very small

- But we are not done yet, we still have to include redshift-space distortions...

Modeling the galaxy power spectrum

- The simplest, linear approach: $P(k, \mu) = (1 + f\mu^2)^2 P_g(k)$...
reference: Kaiser (1987).
- We can include the velocity field to linear order (instead of assuming a linear relation to the density field) $\delta^s(k) = \delta(k) + f\mu^2\theta(k)$, where θ is the divergence of the peculiar velocity field.

$$P_g(k, \mu) = P_{g,\delta\delta}(k) + 2f\mu^2 P_{g,\delta\theta}(k) + f^2\mu^4 P_{\theta\theta}(k)$$

Reference: Scoccimarro (2004)

- On very small scales all perturbation models will break down but it has been shown that an exponential (or Lorentzian) term does a fair job

$$\begin{aligned} P_g(k, \mu) &= \exp(-f^2\sigma_v^2 k^2 \mu^2) \\ &\times [P_{g,\delta\delta}(k) + 2f\mu^2 P_{g,\delta\theta}(k) + f^2\mu^4 P_{\theta\theta}(k)] \end{aligned}$$

- The velocity dispersion term is different for satellites and centrals, so its amplitude very much depends on what galaxies you are trying to model.

Modeling the galaxy power spectrum

- But we still only included the linear correlations between density and velocity divergence. We can go further and include non-linear mappings. Reference: Taruya et al. (2010)

$$\begin{aligned}P_g(k, \mu) = & \exp(-f^2 \sigma_v^2 k^2 \mu^2) \\& \times [P_{g,\delta\delta}(k) + 2f\mu^2 P_{g,\delta\theta}(k) + f^2\mu^4 P_{\theta\theta}(k)] \\& + b_1^3 A(k, \mu, \beta) + b_1^4 B(k, \mu, \beta)\end{aligned}$$

- Terms proportional to b_2 are not even included yet.
- To calculate all the perturbative corrections is computationally expensive and makes a likelihood analysis very challenging.
- Sometimes one can use analytic non-linear power spectrum models calibrated by N-body simulations like halofit (see Smith et al. 2003 and Bird et al. 2012).

One possible outcome of PT

Our power spectrum model is based on renormalized perturbation theory
(Taruya et al. 2011, McDonald & Roy 2009)

$$\begin{aligned} P_g(k, \mu) = & \exp \left\{ - (fk\mu\sigma_v)^2 \right\} [P_{g,\delta\delta}(k) \\ & + 2f\mu^2 P_{g,\delta\theta}(k) + f^2\mu^4 P_{\theta\theta}(k) \\ & + b_1^3 A(k, \mu, \beta) + b_1^4 B(k, \mu, \beta)], \end{aligned}$$

with

$$\begin{aligned} P_{g,\delta\delta}(k) = & b_1^2 P_{\delta\delta}(k) + 2b_2 b_1 P_{b2,\delta}(k) + 2b_{s2} b_1 P_{bs2,\delta}(k) \\ & + 2b_{3\text{nl}} b_1 \sigma_3^2(k) P_m^L(k) + b_2^2 P_{b22}(k) \\ & + 2b_2 b_{s2} P_{b2s2}(k) + b_{s2}^2 P_{bs22}(k) + N, \end{aligned}$$

$$\begin{aligned} P_{g,\delta\theta}(k) = & b_1 P_{\delta\theta}(k) + b_2 P_{b2,\theta}(k) + b_{s2} P_{bs2,\theta}(k) \\ & + b_{3\text{nl}} \sigma_3^2(k) P_m^{\text{lin}}(k), \end{aligned}$$

- Some of the bias parameters are strongly correlated, so we can derive relations using N-body simulations (some model dependency).

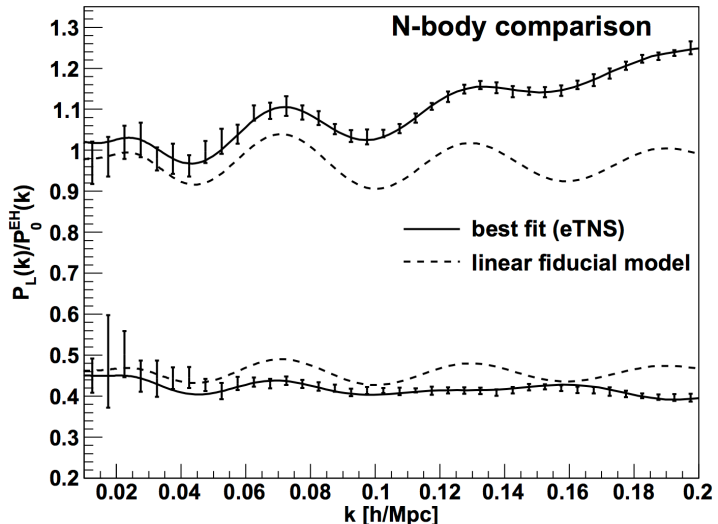
$$b_{s2} = -\frac{4}{7}(b_1 - 1)$$

$$b_{3nl} = -\frac{32}{315}(b_1 - 1)$$

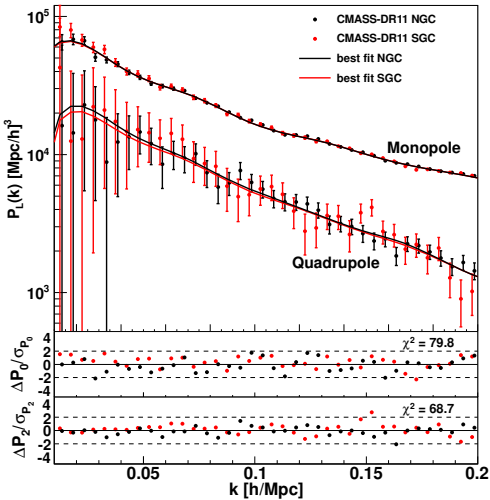
Reference: Saito et al. (2015)

- While the number of modes grows with $\Delta k \propto k^2$, the number of parameters usually also grows... more parameters \rightarrow more degeneracies. But high k region has other powerful observables (e.g. lensing)... Combinations of different observables might break degeneracies.

Power spectrum measurement

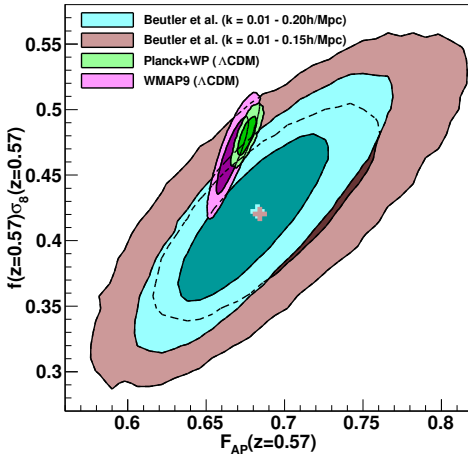


Power spectrum measurements



Beutler et al. (2014)

Power spectrum measurements



Beutler et al. (2014)

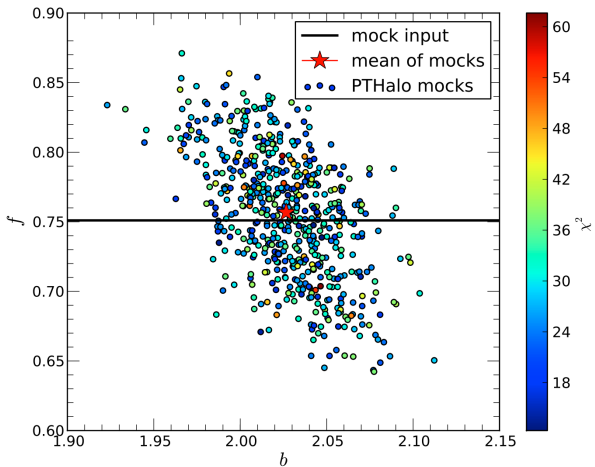
Correlation function modeling

Samushia et al. 2014 uses the model by Reid & White (2011). Convolution of a real-space correlation function template with the probability distribution function of the infall velocity of a galaxy pair along the line-of-sight.

$$1 + \xi^s(r_\sigma, r_\pi) = \int [1 + \xi_g^r(r)] e^{-[r_\pi - y - \mu v_{12}(r)]^2 / 2\sigma_{12}^2(r, \mu)} \frac{dy}{\sqrt{2\pi}\sigma_{12}(r, \mu)}$$

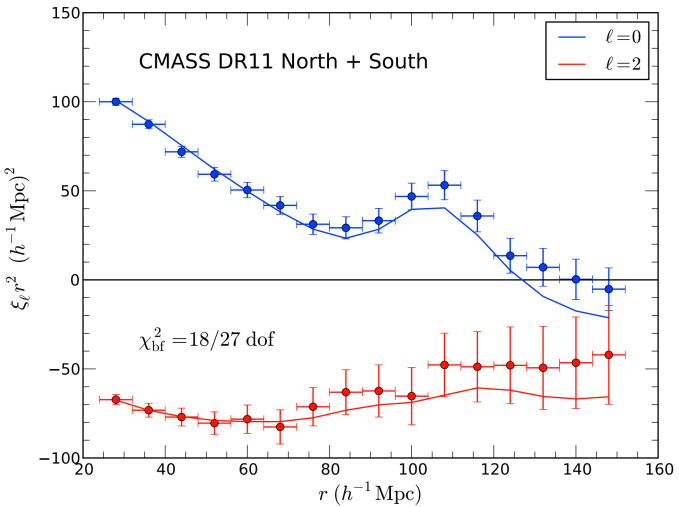
more details in Reid & White (2011)

Configuration-space measurement



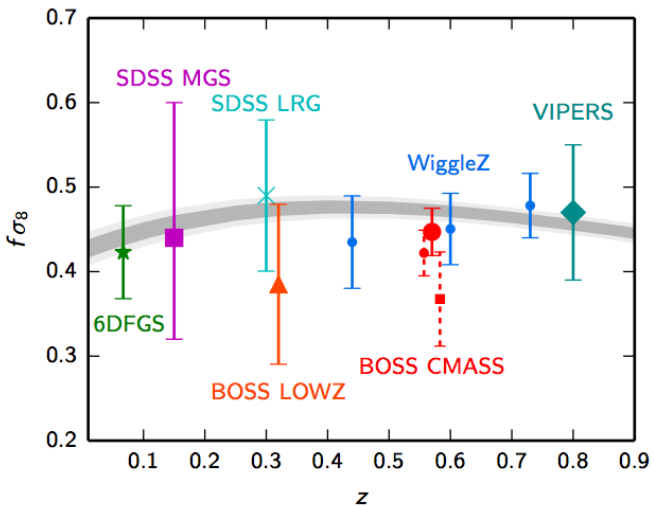
Samushia et al. 2014

Configuration-space measurement



Samushia et al. 2014

Current results



Ade et al. (2015)

Power spectrum measurement

The BOSS-CMASS constraints are:

$$V^{\text{data}} = \begin{pmatrix} D_V(z_{\text{eff}})/r_s(z_d) \\ F_{\text{AP}}(z_{\text{eff}}) \\ f(z_{\text{eff}})\sigma_8(z_{\text{eff}}) \end{pmatrix} = \begin{pmatrix} 13.88 \\ 0.683 \\ 0.422 \end{pmatrix} \quad \begin{matrix} \pm 1.3\% \\ \pm 4.6\% \\ \pm 11\% \end{matrix}$$

where $F_{\text{AP}}(z_{\text{eff}}) = (1 + z_{\text{eff}})D_A(z_{\text{eff}})H(z_{\text{eff}})/c$ at the effective redshift $z_{\text{eff}} = 0.57$. The symmetric covariance matrix between these constraints is given by

$$10^3 C = \begin{pmatrix} 36.400 & -2.0636 & -1.8398 \\ & 1.0773 & 1.1755 \\ & & 1.8478 + 0.196 \end{pmatrix}$$

See Anderson et al. (2014), Beutler et al. (2014), Samushia et al. (2014) and Chuang et al. (2014)

Power spectrum measurement

The BOSS-CMASS constraints are:

$$V^{\text{data}} = \begin{pmatrix} D_V(z_{\text{eff}})/r_s(z_d) \\ F_{\text{AP}}(z_{\text{eff}}) \\ f(z_{\text{eff}})\sigma_8(z_{\text{eff}}) \end{pmatrix} = \begin{pmatrix} 13.88 \\ 0.683 \\ 0.422 \end{pmatrix} \quad \begin{matrix} \pm 1.3\% \\ \pm 4.6\% \\ \pm 11\% \end{matrix}$$

where $F_{\text{AP}}(z_{\text{eff}}) = (1 + z_{\text{eff}})D_A(z_{\text{eff}})H(z_{\text{eff}})/c$ at the effective redshift $z_{\text{eff}} = 0.57$. The symmetric covariance matrix between these constraints is given by

$$10^3 C = \begin{pmatrix} 36.400 & -2.0636 & -1.8398 \\ & 1.0773 & 1.1755 \\ & & 1.8478 + 0.196 \end{pmatrix}$$

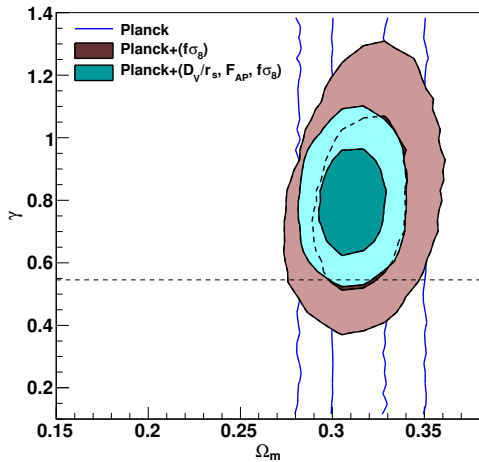
See Anderson et al. (2014), Beutler et al. (2014), Samushia et al. (2014) and Chuang et al. (2014)

→ You can use these constraints to test your own favorite cosmological model.

How do we now test General Relativity?

- Currently there is no obvious/appealing alternative to General Relativity even though the field is very active.
- There are many possible parameterizations for GR.
- Simplest possible test can be done through the γ -parametrization, where $f(z) \approx \Omega_m^\gamma$ and $\gamma_{\text{GR}} \simeq 0.55$.
- But we have measured $f\sigma_8$, not f and what about the background expansion?
- We need the CMB to give us a prior on σ_8 and Ω_m .

Testing GR

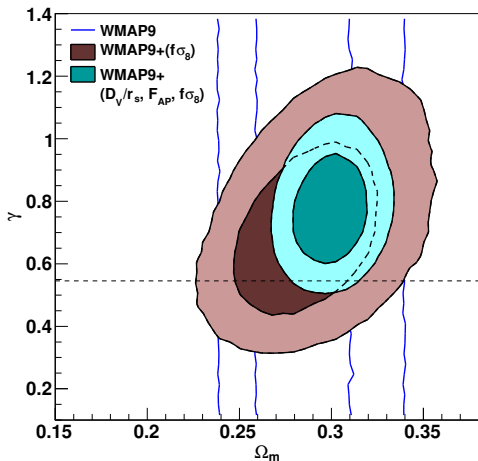


Beutler et al. (2014)

What if we replace Planck with WMAP? WMAP predicts smaller structure growth:

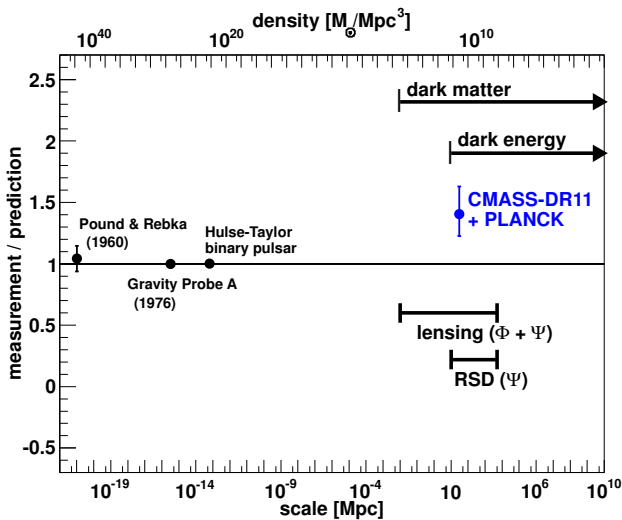
- Planck: $\Omega_m h^2 = 0.1426 \pm 0.0020$, $\Omega_b h^2 = 0.02222 \pm 0.00023$ and $H_0 = 67.31 \pm 0.96$ km/s/Mpc.
Within Λ CDM this predicts $f\sigma_8 = 0.481 \pm 0.010$ at $z = 0.57$.
- WMAP: $\Omega_m h^2 = 0.1364 \pm 0.0050$, $\Omega_b h^2 = 0.02264 \pm 0.00050$ and $H_0 = 70.0 \pm 2.2$ km/s/Mpc.
Within Λ CDM this predicts $f\sigma_8 = 0.451 \pm 0.025$ at $z = 0.57$.

Testing GR



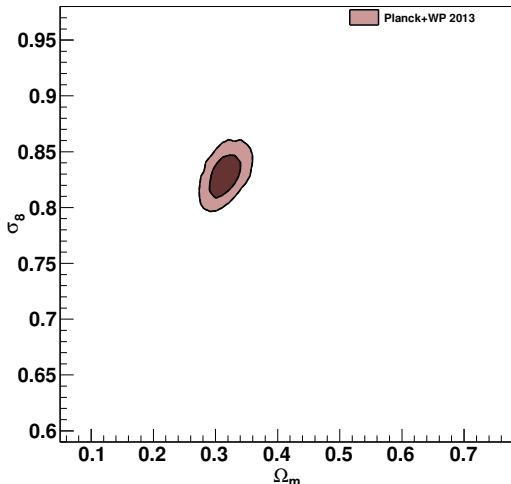
Beutler et al. (2014)

Testing GR



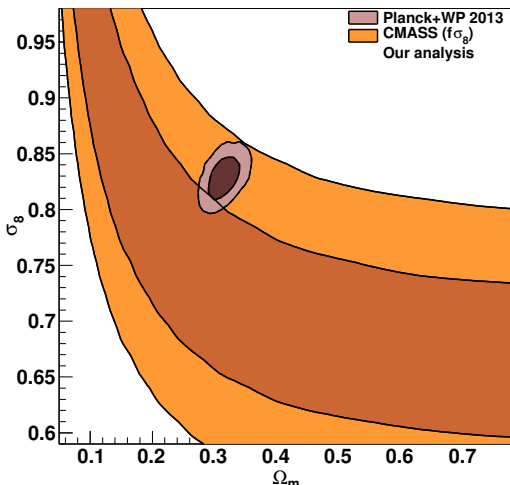
Beutler et al. (2014)

σ_8 - Ω_m likelihood



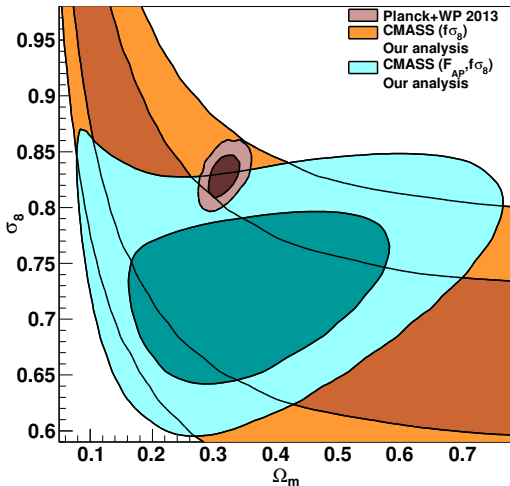
Planck: $\sigma_8 = 0.829 \pm 0.012$

σ_8 - Ω_m likelihood



Planck: $\sigma_8 = 0.829 \pm 0.012$

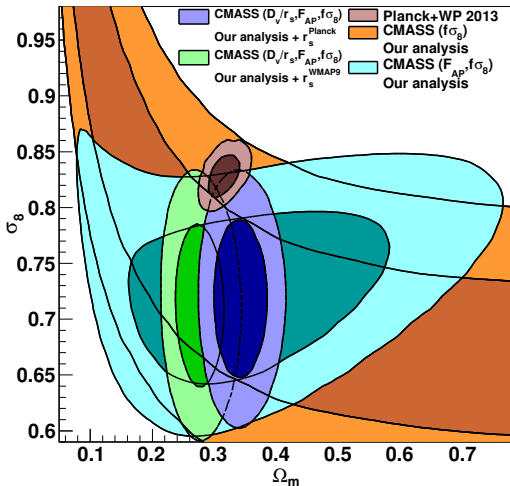
σ_8 - Ω_m likelihood



Planck: $\sigma_8 = 0.829 \pm 0.012$

CMASS: $\sigma_8 = 0.731 \pm 0.052$

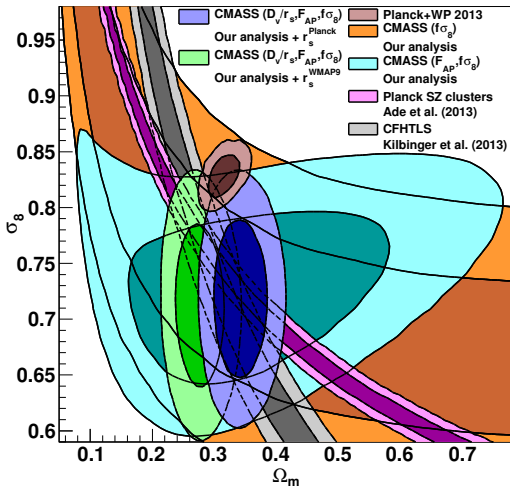
σ_8 - Ω_m likelihood



Planck: $\sigma_8 = 0.829 \pm 0.012$

CMASS: $\sigma_8 = 0.731 \pm 0.052$

σ_8 - Ω_m likelihood



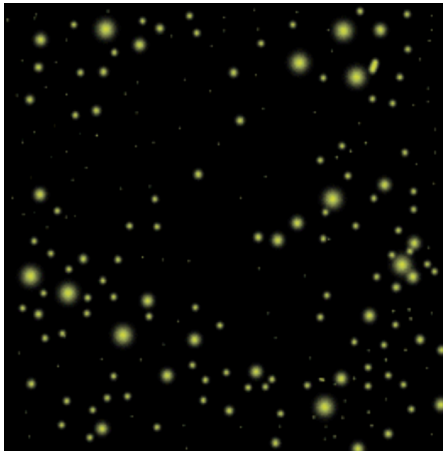
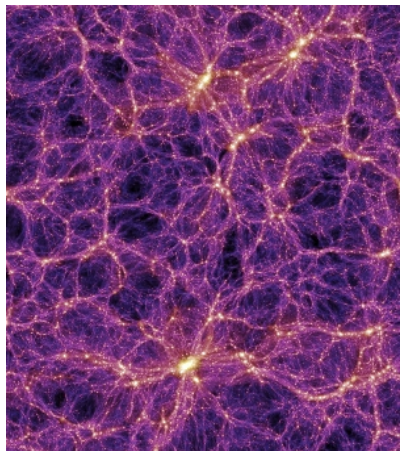
Planck: $\sigma_8 = 0.829 \pm 0.012$

CMASS: $\sigma_8 = 0.731 \pm 0.052$

Conquering the small scales – The halo model

- Galaxies form through the cooling of baryonic material in haloes of dark matter.
- The virial radii of these systems are in excess of 0.1 Mpc, so there is the potential for large differences in the correlation properties of galaxies and dark matter on these scales.
- Currently we have no bias model which can describe the relation between galaxies and dark matter on these small scales.
- The halo model addresses this by creating a density field in which dark-matter haloes are superimposed.
- All the complications of galaxy formation are bypassed via the halo occupation number; the number of galaxies found above some luminosity threshold in a virialized halo of a given mass
- Halo mass determines $P(N_{\text{gal}})$, the probability that a given halo hosts N_{gal} galaxies
- References: Cooray & Sheth (2002), Zehavi et al. (2005)

Conquering the small scales – The halo model



Central assumptions of the halo model

- All dark matter is in halos.
- Correlation functions can be described through correlations within and between halos $\rightarrow \xi(r) = \xi_{1h}(r) + \xi_{2h}(r)$
- Linear theory $P(k)$.
- As input we need
 - A dark matter halo density profile (usually NFW).
 - A halo mass function.
 - A halo bias model.
- The halo occupation distribution $\langle N_{\text{gal}} | M \rangle$ describes how galaxies populate halos.

Conquering the small scales – The halo model

The 1-halo term is given by

$$\xi_{1h} = \frac{1}{\bar{n}_g^2} \int dM \langle N_{\text{gal}}(N_{\text{gal}} - 1)|M\rangle M^2 \frac{dn(M)}{dM} \int d^3x \lambda_M(\vec{x}) \lambda_M(\vec{x} + \vec{r}),$$

where $dn(M)/dM$ is the halo mass function (e.g. Tinker et al. 2010), ρ_M is the mean mass density in the Universe and

$$\lambda_m(r) \sim \left(c_{\text{vir}}(M) \frac{r}{R_{\text{vir}}} \right)^{-1} \left(1 + c_{\text{vir}}(M) \frac{r}{R_{\text{vir}}} \right)^{-2}$$

is the NFW profile. R_{vir} is the virial radius of the halo and $c_{\text{vir}}(M)$ is the mass dependent concentration parameter (e.g. Bullock et al 2001).

Conquering the small scales – The halo model

The 2-halo term is given by

$$\begin{aligned}\xi_{2h} = & \frac{1}{\bar{n}_g^2} \int dM_1 \int dM_2 \langle N_{\text{gal}} | M_1 \rangle M_1 \frac{dn(M_1)}{dM_1} \langle N_{\text{gal}} | M_2 \rangle M_2 \frac{dn(M_2)}{dM_2} \\ & \times \int d^3x \int d^3y \lambda_{M_1}(\vec{x}) \lambda_{M_2}(\vec{y}), \\ & \times \xi_{hh}(\vec{x} - \vec{y} + \vec{r} | M_1, M_2),\end{aligned}$$

where $\xi_{hh}(\vec{x} | M_1, M_2)$ is the cross-correlation function of halos of mass M_1 and M_2 . We can assume that $\xi_{hh}(\vec{x} | M_1, M_2)$ is just a biased version of the linear correlation function $b_h(M_1)b_h(M_2)\xi_{lin}(r)$ and b_h can again be calibrated with simulations (e.g. Tinker et al. 2010).

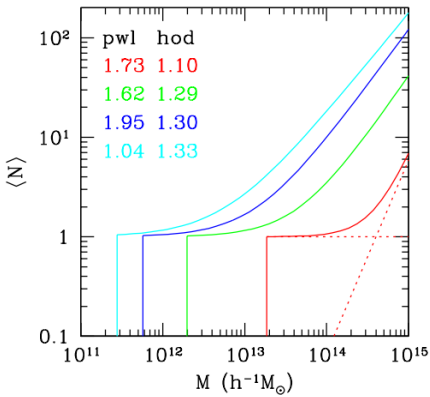
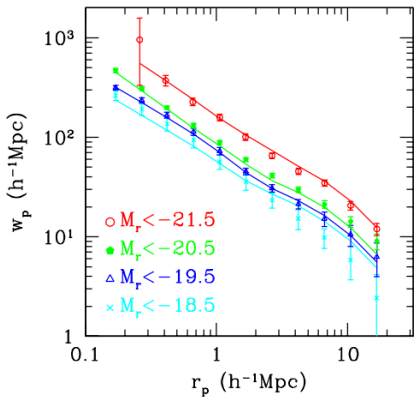
Conquering the small scales – The halo model

- So once the dark matter properties are fixed, the galaxy properties are captured by the HOD.
- $\langle N_{\text{gal}} | M \rangle$ can be as complicated as you want. Usually people divide this in a contribution from satellite galaxies and a contribution from central galaxies. For example one can define:

$$\langle N_{\text{gal}} | M \rangle = \begin{cases} 0 & M < M_{\text{min}} \\ (M/M_{\text{min}})^\alpha & M \geq M_{\text{min}} \end{cases}$$

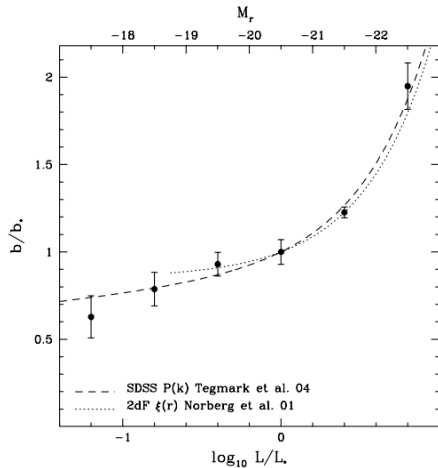
- The halo model is far from perfect. One has many new free parameters to capture non-linear physics, but in general one can't model the correlation function better than 10% on small scales.

Conquering the small scales – The halo model



Zehavi et al. (2005)

Conquering the small scales – The halo model

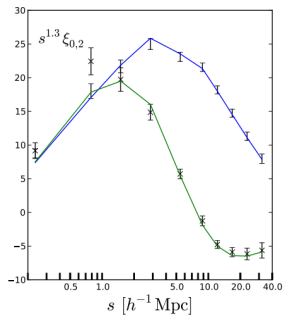
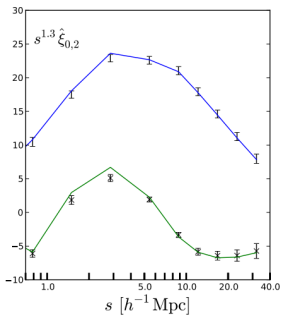
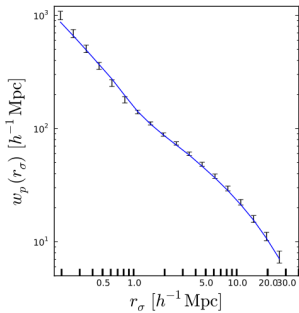


Zehavi et al. (2005)

Conquering the small scales – The halo model

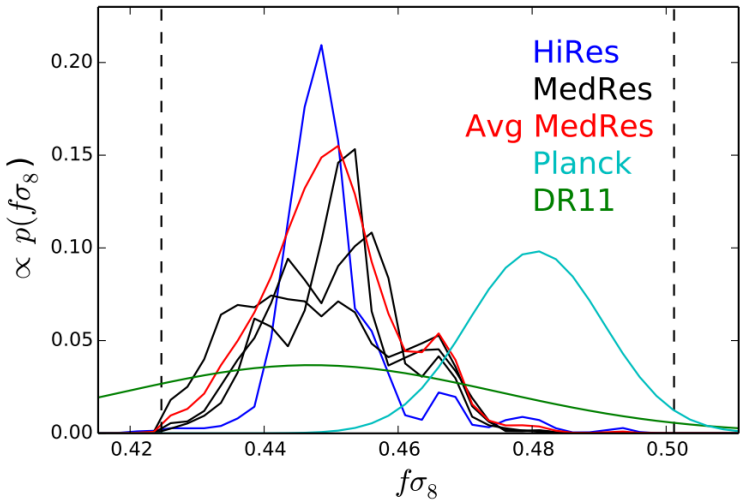
- One primary source of systematic for the study of small scale clustering is fiber collisions.
- Fibers in BOSS cannot be placed closer than $62''$ during one observation.
- Such fiber collisions preferentially happen in high density regions.
- The galaxies which do not get a fiber are a non-random subset of the targets (we also have regions where plates overlap).
- Fiber collisions mainly affect the galaxy clustering on small scales (redshift dependent with $r_{\perp}^{\max} = 0.534$).
- The current solution is a nearest neighbor weighting, which up weights the galaxy closest to the missing galaxy in angular scales. This correction only works if galaxies close to each other in angular scales are really associated in redshift as well. This is true in about 50% of the cases.

Conquering the small scales – The halo model



Reid et al. (2014)

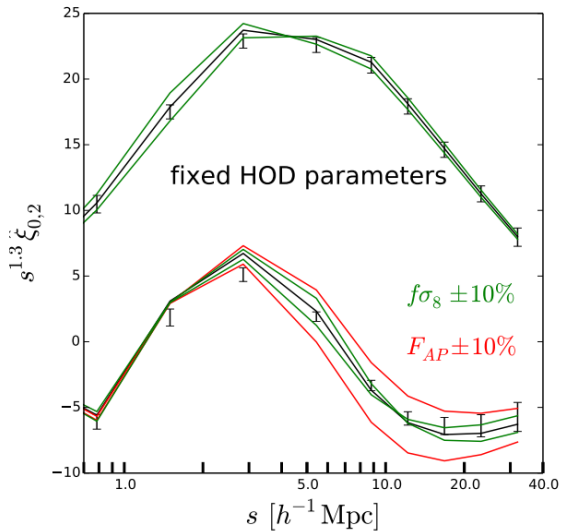
Conquering the small scales – The halo model



$$f\sigma_8 = 0.450 \pm 0.011 \quad (2.5\% \text{ uncertainty})$$

Reid et al. (2014)

Conquering the small scales – The halo model



Reid et al. (2014)

Summary

- Redshift-space distortions introduce an anisotropy in the galaxy clustering (with respect to the line-of-sight).

- Redshift-space distortions introduce an anisotropy in the galaxy clustering (with respect to the line-of-sight).
- Measuring redshift-space distortions allows a constraint on the growth rate $f\sigma_8$.

- Redshift-space distortions introduce an anisotropy in the galaxy clustering (with respect to the line-of-sight).
- Measuring redshift-space distortions allows a constraint on the growth rate $f\sigma_8$.
- To be able to extract the RSD signal we need to understand the shape of the galaxy power spectrum in redshift-space, which is much harder than just modeling the BAO feature.

- Redshift-space distortions introduce an anisotropy in the galaxy clustering (with respect to the line-of-sight).
- Measuring redshift-space distortions allows a constraint on the growth rate $f\sigma_8$.
- To be able to extract the RSD signal we need to understand the shape of the galaxy power spectrum in redshift-space, which is much harder than just modeling the BAO feature.
- Knowing the growth of structure can allow tests of General Relativity on cosmic scales (when combined with priors on the background cosmology).
- There are many ways how one can try to make use of the large number of modes on small scales... e.g. the halo model

There are many more observables in the distribution of galaxies. Two of the most promising are:

- Neutrino mass
- Non-Gaussianity

LSS and the neutrino mass

- At high redshifts, $\Omega_\nu h^2 \sim a^{-4}$ (they are relativistic).
- At lower redshift, $\Omega_\nu h^2 \sim a^{-3}$
- The transition depends on the mass of the neutrinos and is different for the three neutrino eigenstates.
- For a detailed summary see Lesgourgues & Pastor (2006).
- Neutrino oscillation experiments tell us that neutrinos must have a mass.
- Cosmological probes are sensitive to the sum of the neutrino masses $\sum m_\nu$.
- Neutrinos cannot cluster on scales below their free streaming scale

$$k_{\text{FS}} = 0.8 \frac{\sqrt{\Omega_\Lambda + \Omega_m(1+z)^3}}{(1+z)^2} \left(\frac{m_\nu}{1 \text{ eV}} \right) h/\text{Mpc}$$

→ Degeneracy between σ_8 and $\sum m_\nu$ in the CMB.

- The neutrino mass also affects the geometry of the Universe which allows the CMB to break this degeneracy.
- Additional constraints come from gravitational lensing of the CMB.
- The remaining degeneracy can be broken by using low redshift σ_8 constraints.
- We expect similar levels of constraints from upcoming gravitational lensing surveys (like LSST) and CMB lensing, so cosmology should secure a detection of $\sum m_\nu$ in the next decade.
- Current Planck constraint (including lensing): $\sum m_\nu < 0.66 \text{ eV}$ (95% CL.)

LSS and the neutrino mass

So there are two effect we could measure:

- The power spectrum is damped on scales smaller than the free-streaming scale, k_{FS} .

So there are two effect we could measure:

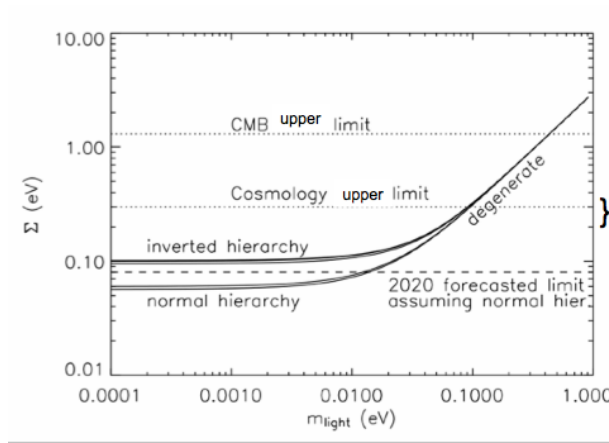
- The power spectrum is damped on scales smaller than the free-streaming scale, k_{FS} .
- The normalization of the power spectrum changes due to the reduction of power on small scales.

$$\sigma_8^2(z) = \int_0^\infty \frac{dk}{2\pi^2} k^2 P(k, z) W^2(k8)$$

where window function is given by $W(k8) = 3j_1(k8)/k8$.

LSS and the neutrino mass

Oscillation experiments so far found that $|\Delta m_{31}^2| \simeq 2.4 \times 10^{-3} \text{ eV}^2$ and $\Delta m_{21}^2 \simeq 7.6 \times 10^{-5} \text{ eV}^2$ (Beringer et al. 2012). Therefore knowing the sum of the neutrino masses will determine the mass hierarchy.

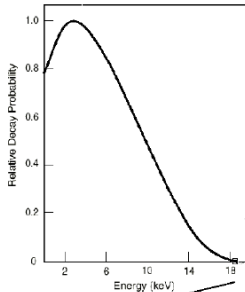
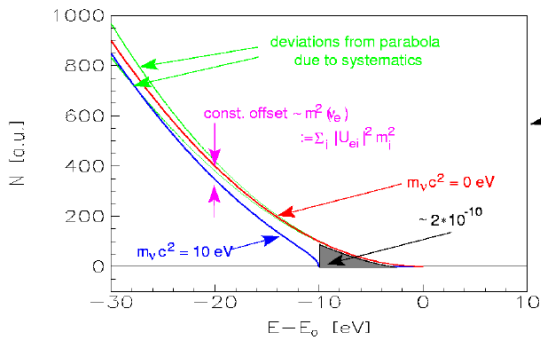


Tritium β decay spectrum

superallowed



$t_{1/2}: 12.3 \text{ y}$

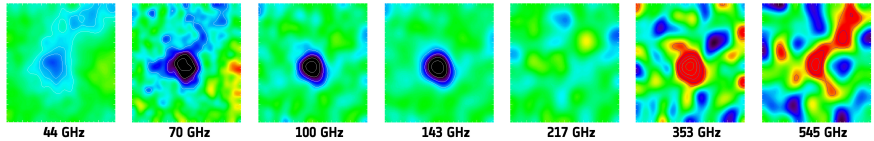


- Clusters
- The shape of the galaxy power spectrum.
- The Ly- α forest.

Neutrino mass constraints from the SZ cluster counts

- The Sunyaev-Zel'dovich effect (SZ) is the result of high energy electrons distorting the cosmic microwave background radiation (CMB) through inverse Compton scattering, in which the low energy CMB photons receive an average energy boost during collision with the high energy cluster electrons. These electron-photon collisions redistribute the frequencies of photons in a characteristic way such that, when looking at the CMB in the direction of a galaxy cluster, one observes a deficit, with respect to the average CMB signal, of low-energy photons, and a subsequent surplus of more energetic ones. In other words, along the line of sight of a galaxy cluster, the CMB appears fainter at low frequencies and brighter at high frequencies, with the transition value corresponding to 217 GHz.
- Since the Sunyaev-Zel'dovich effect is a scattering effect, its magnitude is independent of redshift. This means that clusters at high redshift can be detected just as easily as those at low redshift (but depending on the survey sensitivity).

Neutrino mass constraints from the SZ cluster counts



- Currently best constraints from Planck, Ade et al. (2015)
- 439 clusters detected through the Sunyaev-Zeldovich (SZ) signal... but statistics is not the main aspect to worry about.
- It seems that all experiments which try to find clusters using the SZ effect see far fewer clusters than predicted by Λ CDM.
- The cluster mass scale is the largest source of uncertainty in interpreting the observed cluster counts. We can estimate the cluster mass through:
 - weak lensing (independent of the dynamical state of the cluster)... von der Linden et al. (2014)
 - CMB lensing (available for all clusters, not just a sub-sample)
- Cluster abundance is a function of halo mass and redshift as specified by the mass function.

Neutrino mass constraints from the SZ cluster counts

The predicted number of clusters is

$$n_i = \int_{z_i}^{z_{i+1}} dz \frac{dN}{dz}$$

with

$$\frac{dN}{dz} = \int d\Omega \int dM_{500} \chi(z, M_{500}, l, b) \frac{dN}{dz dM_{500} d\Omega}$$

where χ is the survey completeness at a given position on the sky (l, b) and M_{500} is the mass within the radius where the mean enclosed density is 500 times the critical density.

Neutrino mass constraints from the SZ cluster counts

- The observed flux can be related to the mass using scaling relations which have been established by X-ray observations.
- Such mass determinations rely on hydrostatic equilibrium of the intra-cluster gas and deviations from that assumption are parametrized through the bias parameter b (biggest source of uncertainty $\sim 30\%$). This could also depend on z and mass...

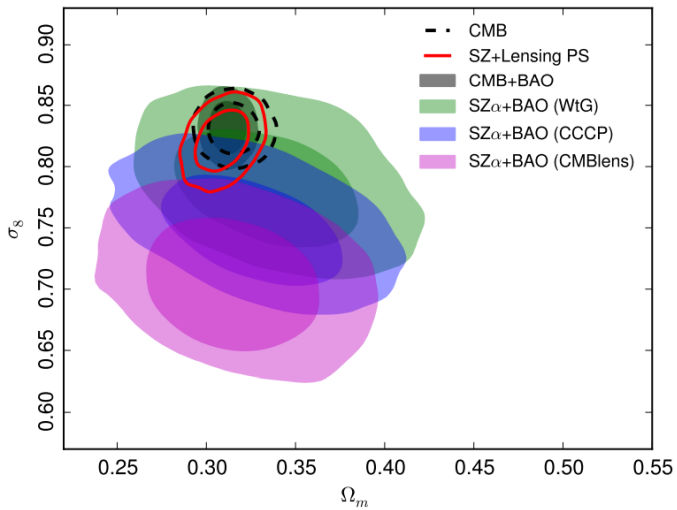
Prior name	Quantity	Value & Gaussian errors
Weighing the Giants (WtG)	$1 - b$	0.688 ± 0.072
Canadian Cluster Comparison Project (CCCP)	$1 - b$	0.780 ± 0.092
CMB lensing (LENS)	$1/(1 - b)$	0.99 ± 0.19
Baseline 2013	$1 - b$	$0.8 [-0.1, +0.2]$

Ade et al. (2015)

In general, the mass bias could depend on cluster mass and redshift, although we will model it by a constant in the following. Our motivation is one of practicality: the limited size and precision of current lensing samples makes it difficult to constrain any more than a constant, i.e., the overall mass scale of our catalogue. Large lensing surveys like *Euclid*, WFIRST, and the Large Synoptic Survey Telescope, and CMB lensing will improve this situation in coming years.

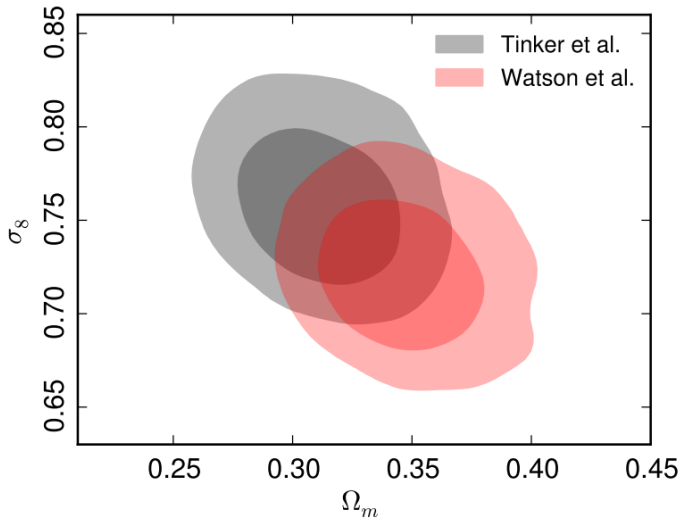
Ade et al. (2015)

Neutrino mass constraints from the SZ cluster counts



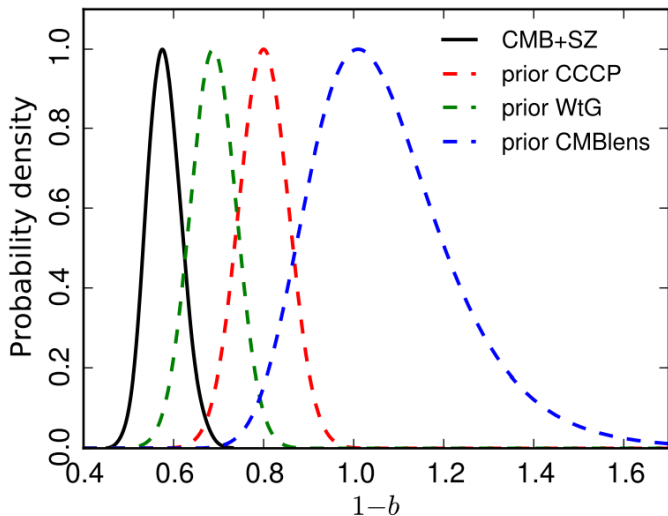
Ade et al. (2015)

Neutrino mass constraints from the SZ cluster counts



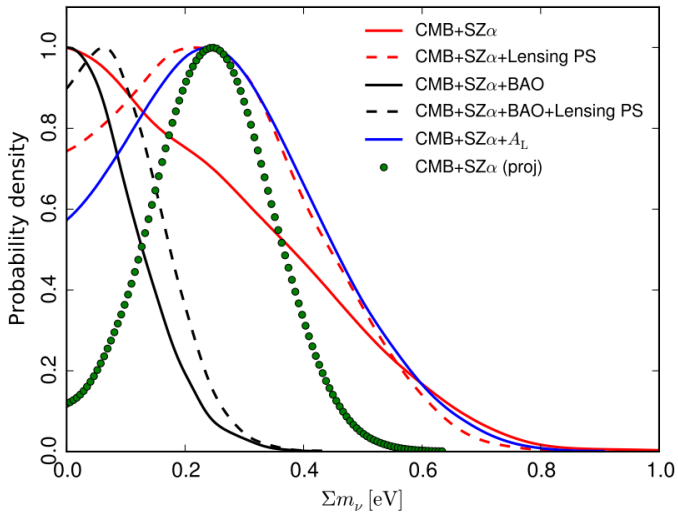
Ade et al. (2015)

Neutrino mass constraints from the SZ cluster counts



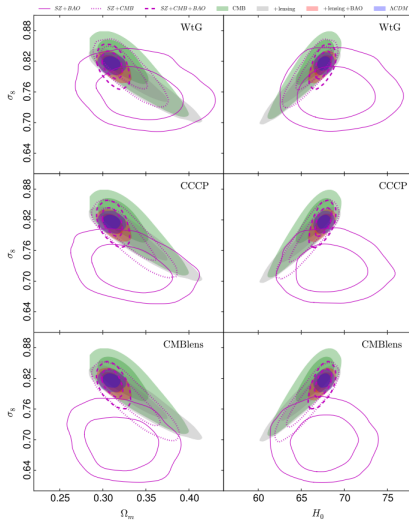
Ade et al. (2015)

Neutrino mass constraints from the SZ cluster counts



Ade et al. (2015)

Neutrino mass constraints from the SZ cluster counts



Ade et al. (2015)

- There are various sources of systematic uncertainties in this sort of measurement.
- All current priors on $1 - b$ cannot account for the tension with the primary CMB, which would require $1 - b = 0.58 \pm 0.04$. The WtG project is closest.
- SPT and ACT are in broad agreement with the Planck results.
- The neutrino mass is not able to solve the tension, because it would also require a smaller Hubble constant and larger Ω_m .

Neutrino mass constraints from the power spectrum shape

How can we model the shape of the power spectrum including the effect of neutrinos?

Following the method used in Zhao et al. (2014), BOSS-DR9 analysis:

- To first order we can assume that neutrino perturbations are linear (see Saito et al. 2009).
- We can then write the power spectrum model as

$$P_{cb\nu}(k) = f^2 P_{cb}^L(k) + 2f_{cb}f_\nu P_{cb\nu}^L(k) + f_\nu^2 P_\nu^L(k)$$

where

$$f_\nu = \frac{\Omega_\nu}{\Omega_m}$$

$$f_{cb} = 1 - f_\nu$$

- However, we measure the galaxy power spectrum, not the matter power spectrum. So we need to include a galaxy bias:

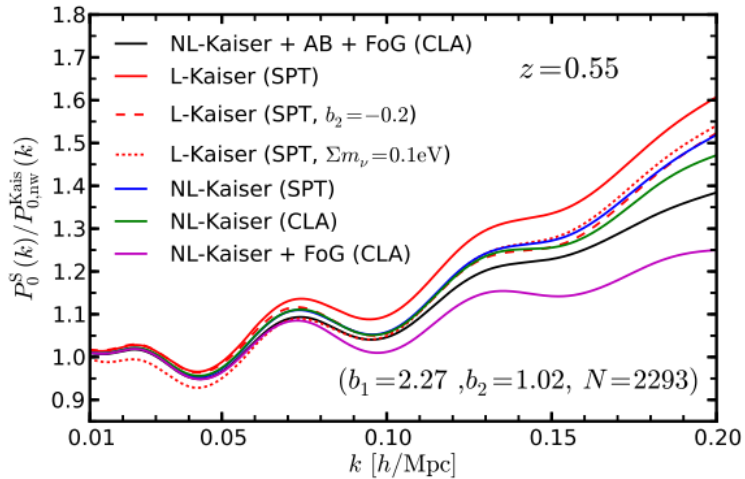
$$P_g(k) = b_1^2 [P_{cb\nu}(k) + b_2 P_{b2}(k) + b_2^2 P_{b22}(k)] + N$$

- But we still only included the linear correlations between density and velocity divergence. We can go further and include non-linear mappings. Reference: Taruya et al. (2010)

$$\begin{aligned} P_g(k, \mu) = & \exp(-f^2 \sigma_v^2 k^2 \mu^2) \\ & \times [P_{g,\delta\delta}(k) + 2f\mu^2 P_{g,\delta\theta}(k) + f^2\mu^4 P_{\theta\theta}(k)] \\ & + b_1^3 A(k, \mu, \beta) + b_1^4 B(k, \mu, \beta) \end{aligned}$$

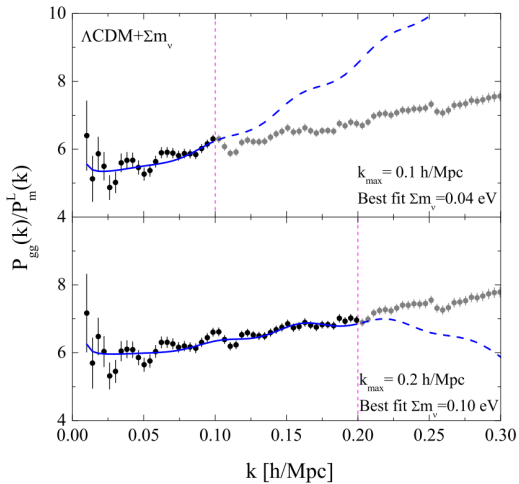
- Terms proportional to b_2 are not even included yet.
- To calculate all the perturbative corrections is computationally expensive and makes a likelihood analysis very challenging.
- Sometimes one can use analytic non-linear power spectrum models calibrated by N-body simulations like halofit (see Smith et al. 2003 and Bird et al. 2012).

Neutrino mass constraints from the power spectrum shape



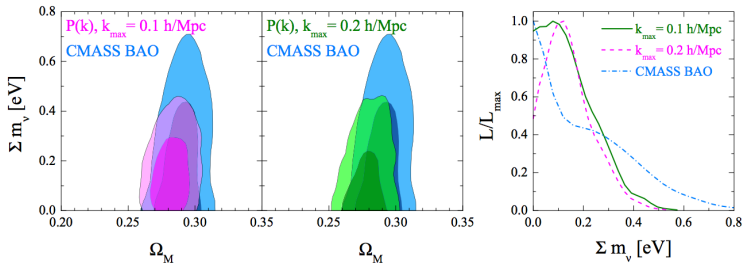
Zhao et al. (2014)

Neutrino mass constraints from particle physics



Zhao et al. (2014)

Neutrino mass constraints from the power spectrum shape



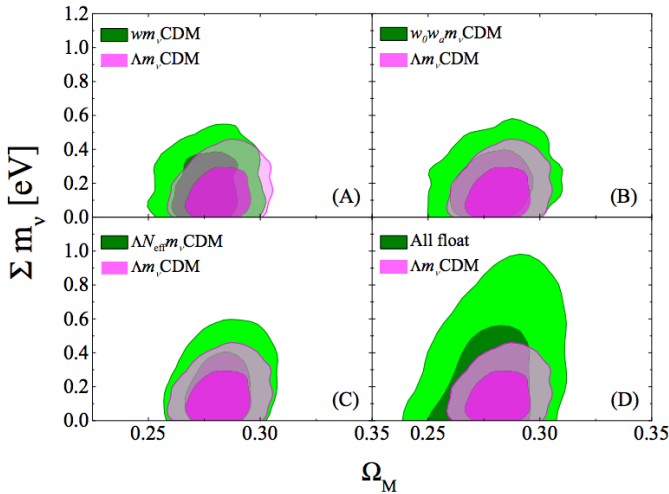
$\sum m_\nu < 0.340 \text{ eV}$ (WMAP7 + SNLS3 + CMASS)

$\sum m_\nu < 0.334 \text{ eV}$ (WMAP7 + SNLS3 + CMASS)

Zhao et al. (2014)

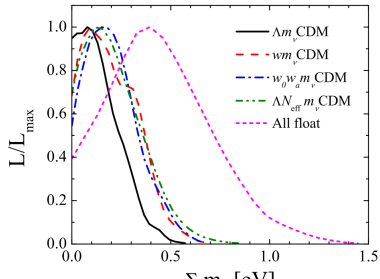
Neutrino mass constraints from the power spectrum shape

What about the background cosmology?



Zhao et al. (2014)

Neutrino mass constraints from the power spectrum shape



$$\Lambda m_\nu \text{ CDM}: \sum m_\nu < 0.340 \text{ eV}$$

$$\Lambda m_\nu N_{\text{eff}} \text{ CDM}: \sum m_\nu < 0.491 \text{ eV}$$

$$w m_\nu \text{ CDM}: \sum m_\nu < 0.432 \text{ eV}$$

$$w_0 w_a m_\nu \text{ CDM}: \sum m_\nu < 0.618 \text{ eV}$$

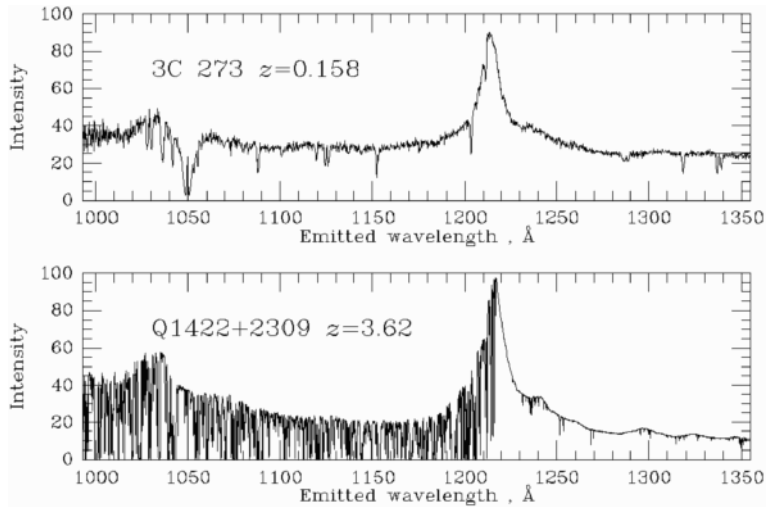
$$\Lambda m_\nu \alpha_s \text{ CDM}: \sum m_\nu < 0.395 \text{ eV}$$

$$\text{All float}: \sum m_\nu < 0.821 \text{ eV}$$

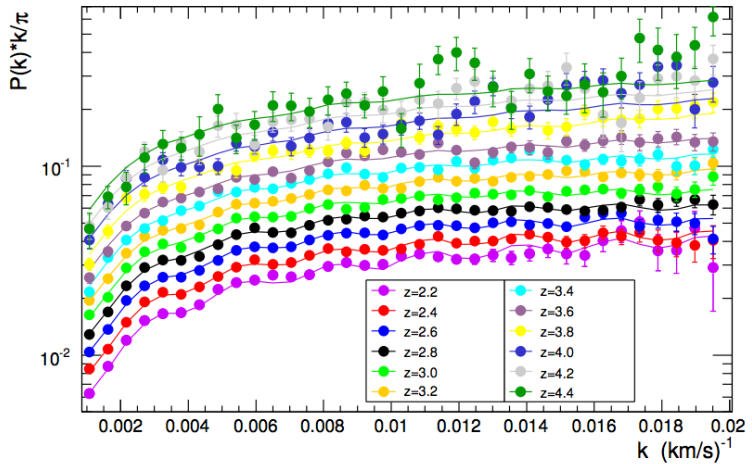
Zhao et al. (2014)

- The Ly- α forest is also sensitive to the neutrino mass... here we follow Palanque-Delabrouille et al. (2015).
- Strongest cosmological bound to date $\sum m_\nu < 0.15 \text{ eV}$ (95% CL.)
- Close to the scale where it can distinguish between the neutrino hierarchy...
- The Ly- α forest allows the measurement of the one-dimensional flux power spectrum, which is related to the underlying three-dimensional matter power spectrum.
- The Ly- α power spectrum is completely non-linear, but we can run hydro simulations to understand this non-linear power spectrum. For galaxies we can't do that, since we would need to understand halo and galaxy formation.

Neutrino mass constraints from the Lyman- α forest



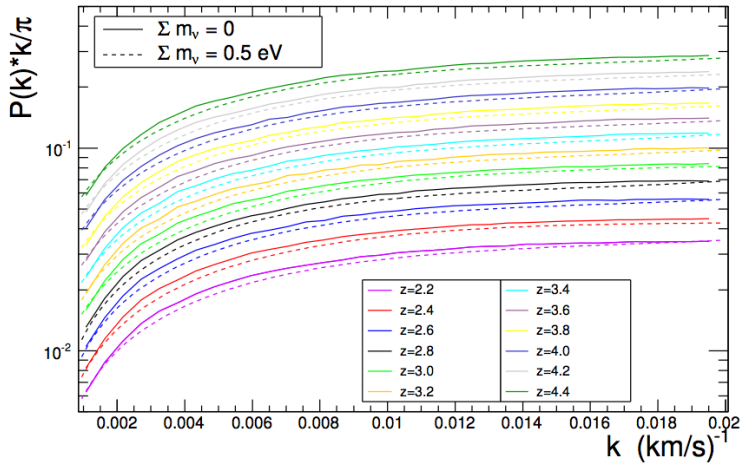
Neutrino mass constraints from the Lyman- α forest



Palanque-Delabrouille et al. (2015)

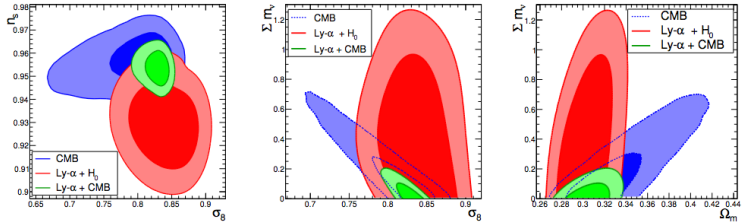
- One has to run hydrodynamical simulations. In this analysis the following parameters have been varied in the simulations
 - $n_s = 0.96 \pm 0.05$
 - $\sigma_8 = 0.83 \pm 0.05$
 - $\Omega_m = 0.31 \pm 0.05$
 - $H_0 = 67.5 \pm 5 \text{ km/s/Mpc}$
 - $T_0(z=3) = 14000 \pm 7000$
 - $\gamma(z=3) = 1.3 \pm 0.3$
 - $A^\tau = 0.0025 \pm 0.0020$ (posteriori)
 - $\eta^\tau = 3.7 \pm 0.4$ (posteriori)
 - $\sum m_\nu = 0/0.4/0.8 \text{ eV}$
 - + 19 astrophysical and nuisance parameters
- T and γ are related to the heating rate of the intergalactic medium.
- The Ly- α data prefer the highest values of σ_8 compatible with the CMB data.

Neutrino mass constraints from the Lyman- α forest



Palanque-Delabrouille et al. (2015)

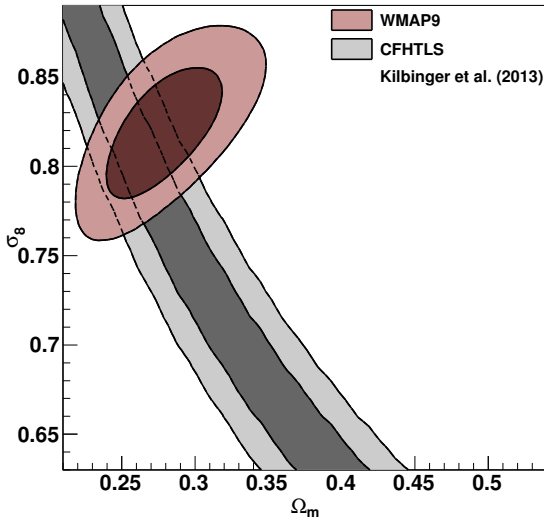
Neutrino mass constraints from the Lyman- α forest



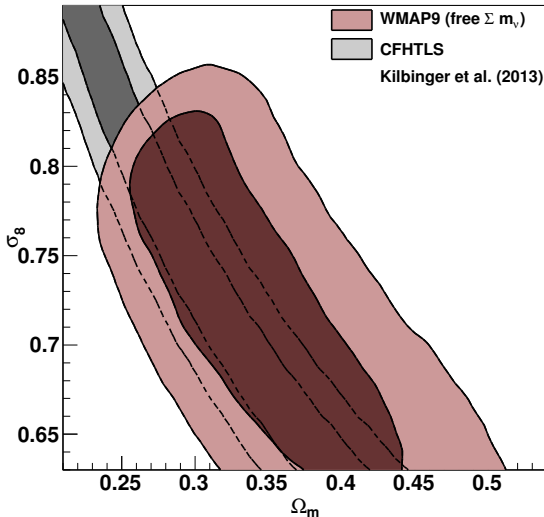
Parameter	Ly α + H_0^{Gaussian} ($H_0 = 67.4 \pm 1.4$)	Ly α + Planck	Ly α + CMB	Ly α + CMB + BAO	Ly α + WMAP9 + ACT + SPT
n_s	0.928 ± 0.012	0.958 ± 0.006	0.954 ± 0.005	0.954 ± 0.005	0.950 ± 0.007
H_0 (km s $^{-1}$ Mpc $^{-1}$)	67.2 ± 1.4	67.9 ± 1.0	68.0 ± 1.0	67.8 ± 0.5	67.8 ± 1.1
$\sum m_\nu$ (eV)	< 1.1 (95%)	< 0.22 (95%)	< 0.15 (95%)	< 0.14 (95%)	< 0.31 (95%)
σ_8	0.846 ± 0.039	0.822 ± 0.018	0.832 ± 0.009	0.837 ± 0.011	0.789 ± 0.025
Ω_m	0.296 ± 0.017	0.296 ± 0.016	0.303 ± 0.014	0.308 ± 0.007	0.288 ± 0.016

Palanque-Delabrouille et al. (2015)

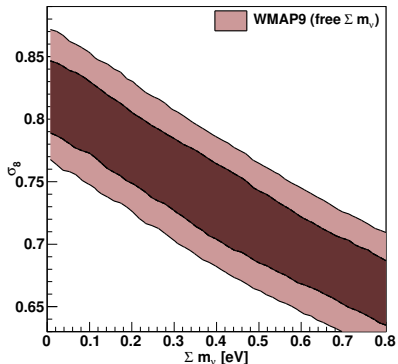
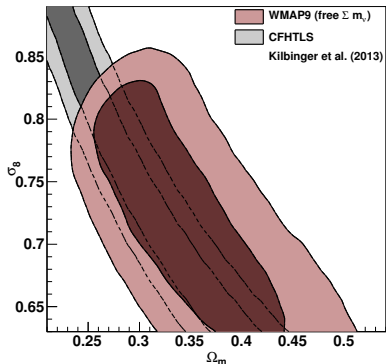
Neutrino mass constraints from the growth rate



Neutrino mass constraints from the growth rate

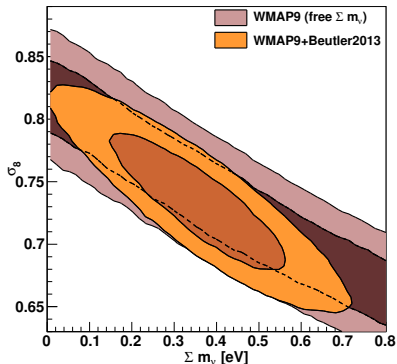
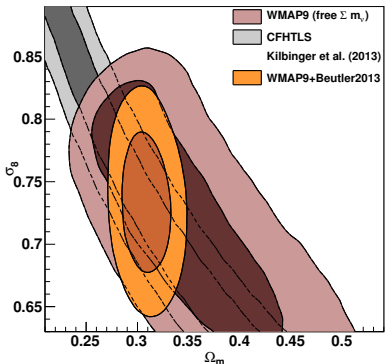


Neutrino mass constraints from the growth rate



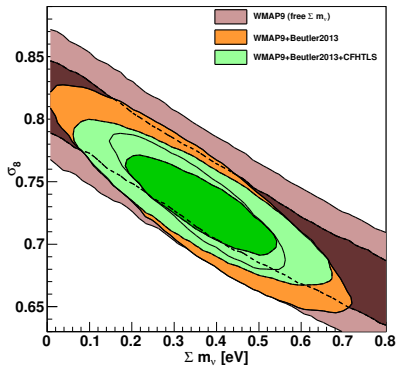
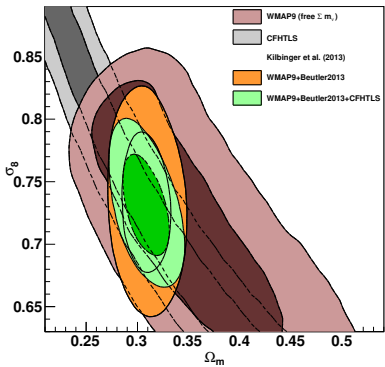
dataset(s)	$\sum m_\nu$ [eV] 68% c.l.	$\sum m_\nu$ [eV] 95% c.l.
WMAP9	< 0.75	< 1.3

Neutrino mass constraints from the growth rate



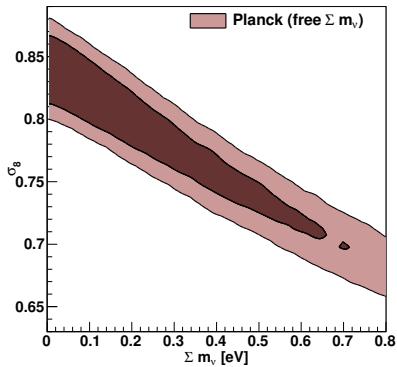
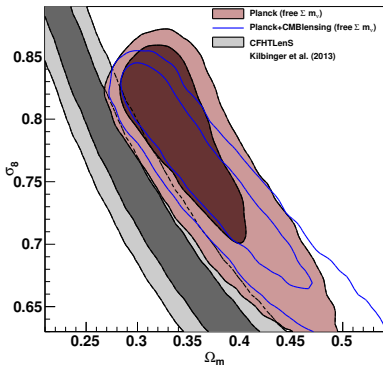
dataset(s)	$\sum m_\nu$ [eV]	
	68% c.l.	95% c.l.
WMAP9	< 0.75	< 1.3
WMAP9+CMASS	0.36 ± 0.14	0.36 ± 0.28

Neutrino mass constraints from the growth rate



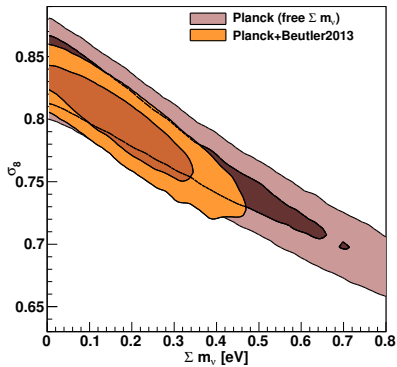
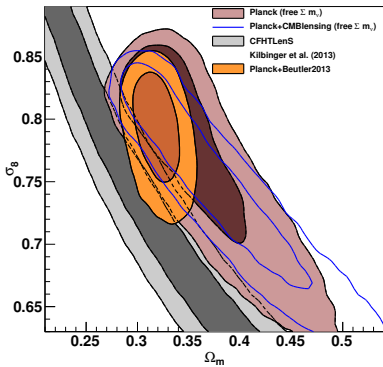
dataset(s)	$\sum m_\nu$ [eV]	
	68% c.l.	95% c.l.
WMAP9	< 0.75	< 1.3
WMAP9+CMASS	0.36 ± 0.14	0.36 ± 0.28
WMAP9+CMASS+CFHTLenS	0.37 ± 0.12	0.37 ± 0.24

Neutrino mass constraints from the growth rate



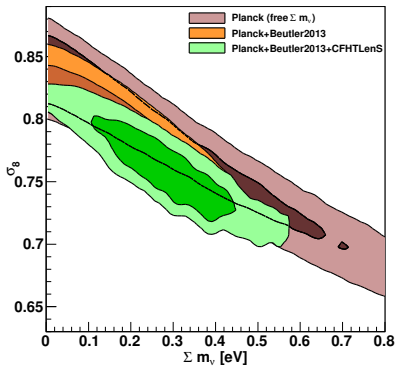
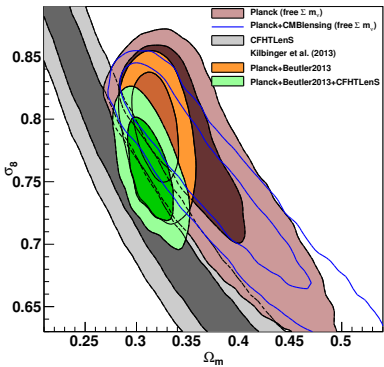
dataset(s)	$\sum m_\nu$ [eV] 68% c.l.	$\sum m_\nu$ [eV] 95% c.l.
Planck	< 0.41	< 0.95

Neutrino mass constraints from the growth rate



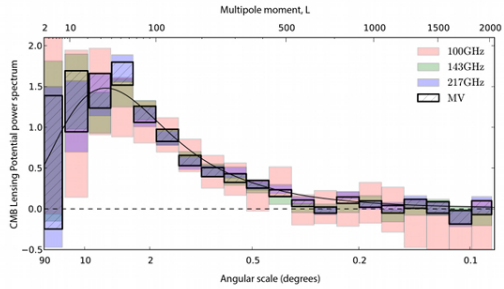
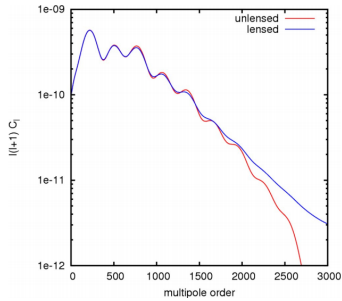
dataset(s)	$\sum m_\nu$ [eV]	
	68% c.l.	95% c.l.
Planck	< 0.24	< 0.67
Planck+CMASS	0.20 ± 0.13	< 0.40

Neutrino mass constraints



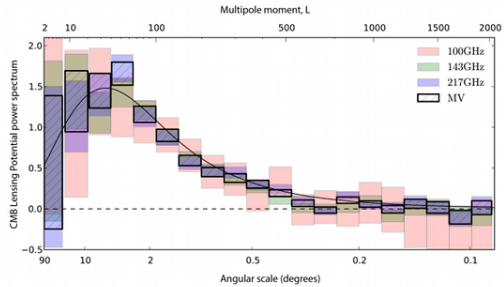
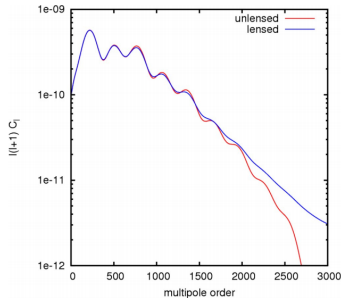
dataset(s)	$\sum m_\nu$ [eV]	
	68% c.l.	95% c.l.
Planck	< 0.24	< 0.67
Planck+CMASS	0.20 ± 0.13	< 0.40
Planck+CMASS+CFHTLenS	0.29 ± 0.13	$0.29^{+0.29}_{-0.23}$

Lensing contribution to Planck



credit: Planck col.

Lensing contribution to Planck



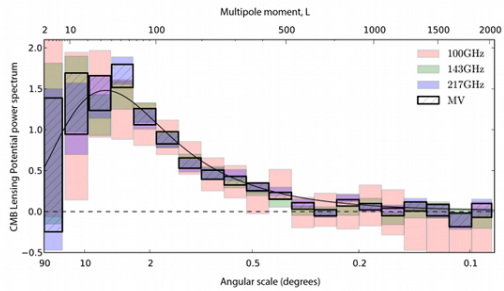
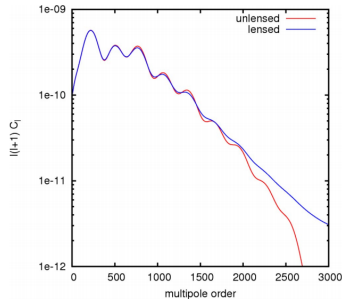
credit: Planck col.

$$T^{\text{lensed}}(\hat{n}) = T^{\text{unlensed}}(\hat{n} + \nabla\phi(\hat{n}))$$

with the CMB lensing potential

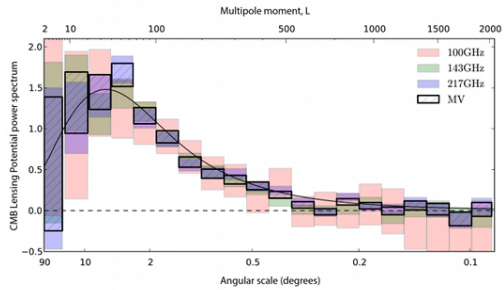
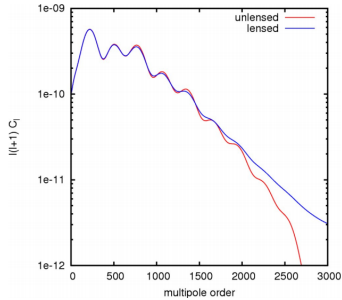
$$\phi(\hat{n}) = -2 \int_0^{\chi(z_*)} d\chi \frac{\chi(z_*) - \chi}{\chi(z_*) \chi} \Psi(\chi \hat{n}, \eta_0 - \chi)$$

Lensing contribution to Planck



credit: Planck col.

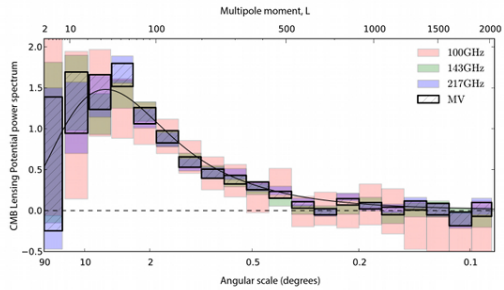
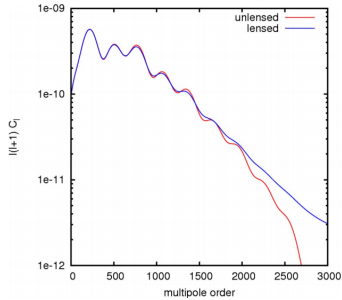
Lensing contribution to Planck



credit: Planck col.

- Lensing leads to a damping of the high ℓ peaks in the temperature power spectrum

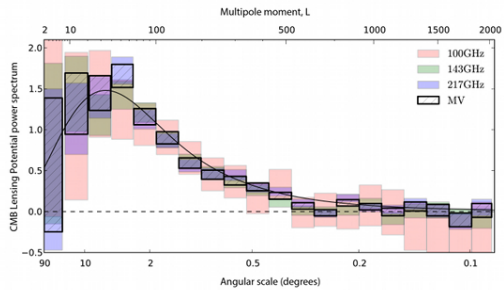
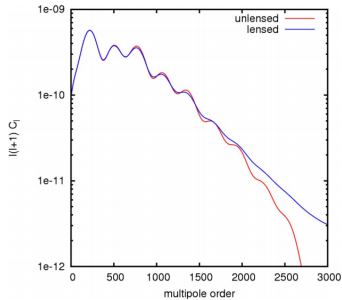
Lensing contribution to Planck



credit: Planck col.

- Lensing leads to a damping of the high ℓ peaks in the temperature power spectrum $\rightarrow 10\sigma$ detection.

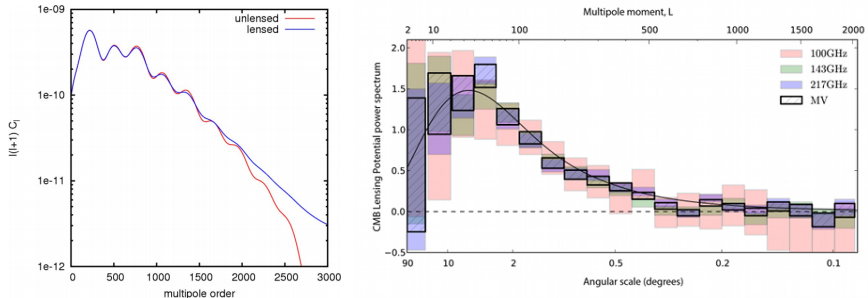
Lensing contribution to Planck



credit: Planck col.

- Lensing leads to a damping of the high ℓ peaks in the temperature power spectrum $\rightarrow 10\sigma$ detection.
- Gravitational lensing introduces non-Gaussianity into the CMB fluctuations, which can be measured with the 4-point function or trispectrum

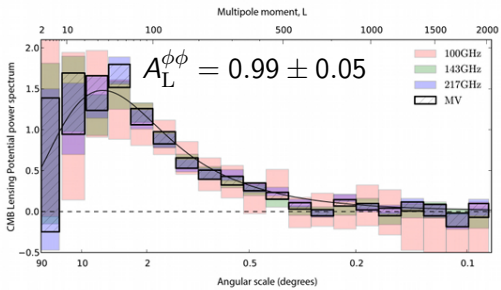
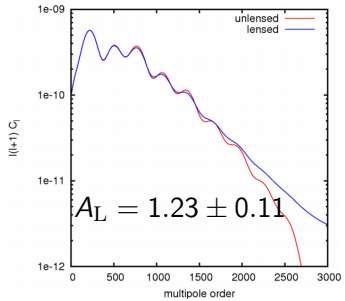
Lensing contribution to Planck



credit: Planck col.

- Lensing leads to a damping of the high ℓ peaks in the temperature power spectrum $\rightarrow 10\sigma$ detection.
- Gravitational lensing introduces non-Gaussianity into the CMB fluctuations, which can be measured with the 4-point function or trispectrum $\rightarrow 25\sigma$ detection.

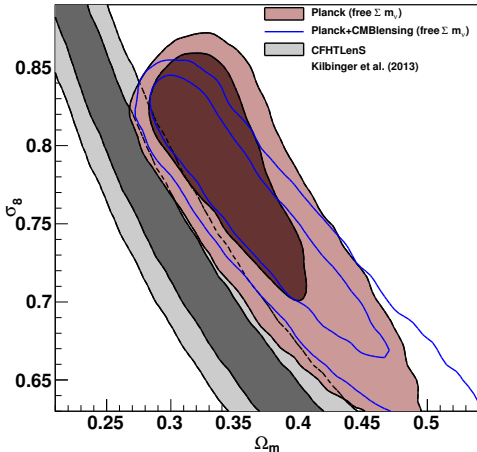
Lensing contribution to Planck



credit: Planck col.

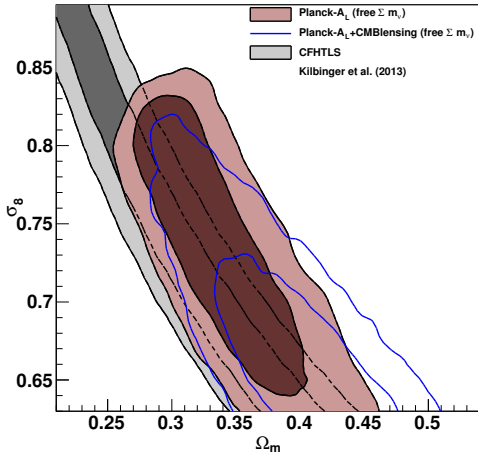
- Lensing leads to a damping of the high ℓ peaks in the temperature power spectrum $\rightarrow 10\sigma$ detection.
- Gravitational lensing introduces non-Gaussianity into the CMB fluctuations, which can be measured with the 4-point function or trispectrum $\rightarrow 25\sigma$ detection.

Lensing contribution to Planck



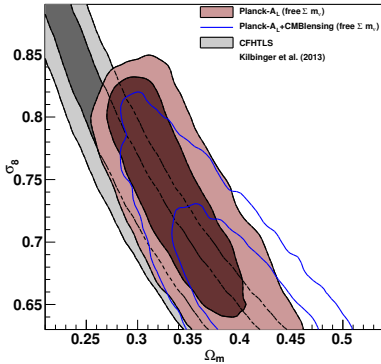
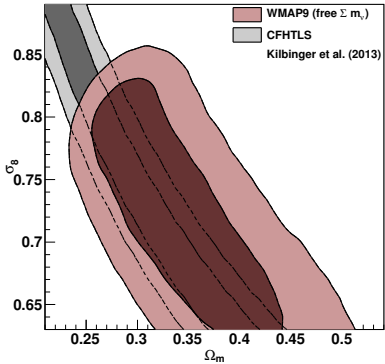
See Planck collaboration XVI section 5.1

Lensing contribution to Planck

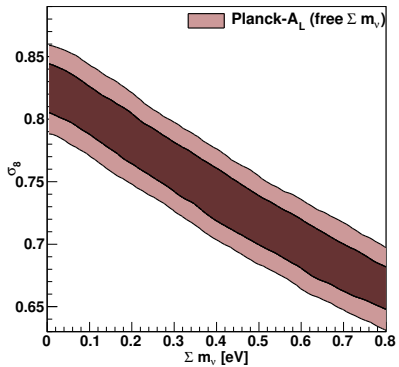
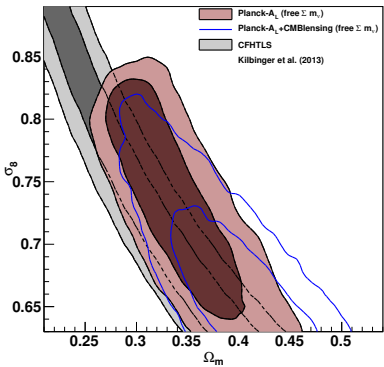


See Planck collaboration XVI section 5.1

Lensing contribution to Planck

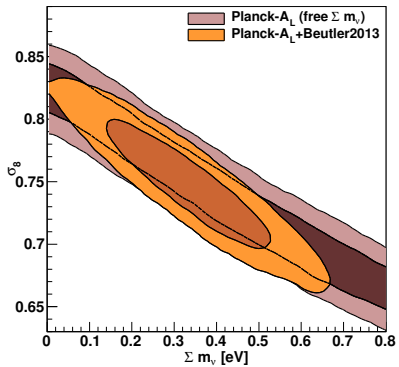
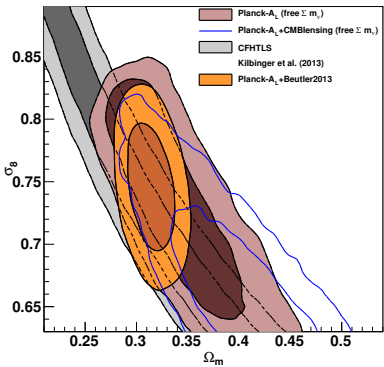


Neutrino mass constraints



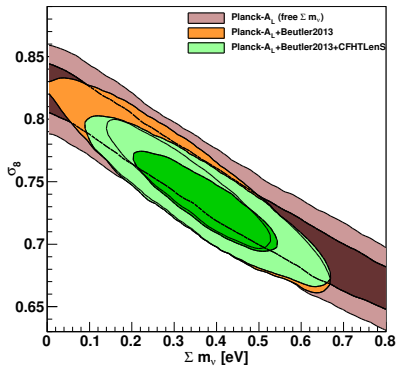
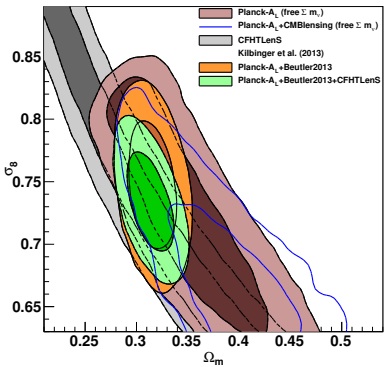
dataset(s)	$\sum m_\nu$ [eV] 68% c.l.	$\sum m_\nu$ [eV] 95% c.l.
Planck-A _L	< 0.71	< 1.2

Neutrino mass constraints



dataset(s)	$\sum m_\nu$ [eV] 68% c.l.	$\sum m_\nu$ [eV] 95% c.l.
Planck- A_L	< 0.71	< 1.2
Planck- A_L +CMASS	0.34 ± 0.14	0.34 ± 0.26

Neutrino mass constraints



dataset(s)	$\sum m_\nu$ [eV]	
	68% c.l.	95% c.l.
Planck-A _L	< 0.71	< 1.2
Planck-A _L +CMASS	0.34 ± 0.14	0.34 ± 0.26
Planck-A _L +CMASS+CFHTLenS	0.38 ± 0.11	0.38 ± 0.24

Summary:

- There is tension between WMAP9 and Planck, which has a significant impact on the neutrino mass constraints.

Summary:

- There is tension between WMAP9 and Planck, which has a significant impact on the neutrino mass constraints.

dataset(s)	$\sum m_\nu$ [eV]	
	68% c.l.	95% c.l.
WMAP9+CMASS	0.36 ± 0.14	0.36 ± 0.28
Planck+CMASS	0.20 ± 0.13	< 0.37
Planck-A _L +CMASS	0.34 ± 0.14	0.34 ± 0.26

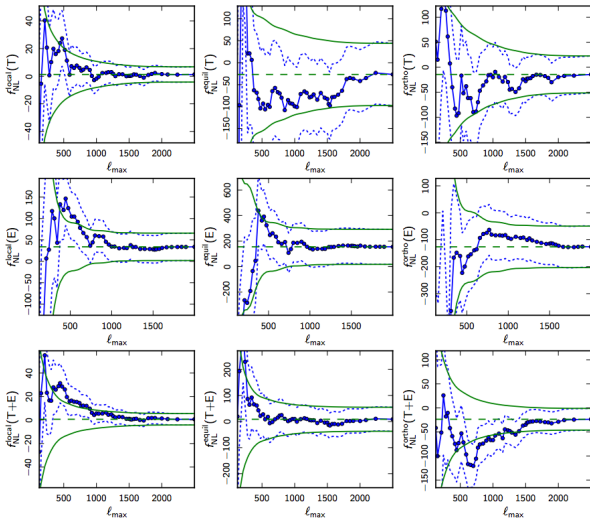
dataset(s)	$\sum m_\nu$ [eV]	
	68% c.l.	95% c.l.
WMAP9+CMASS+CFHTLenS	0.37 ± 0.12	0.37 ± 0.24
Planck+CMASS+CFHTLenS	0.29 ± 0.13	$0.29^{+0.29}_{-0.23}$
Planck-A _L +CMASS+CFHTLenS	0.38 ± 0.11	0.38 ± 0.24

Summary, neutrino mass

- The neutrino mass damps the clustering amplitude below the free-streaming scale.
- There are many ways in which we can try to measure this effect from cosmology (RSD, power spectrum shape, CMB lensing, Ly- α forest...). Confirmation will be needed for a believable detection.
- Currently there are no clear detections of the neutrino mass and chances are that the neutrino mass is close to the minimum mass.
- The next generation of cosmological experiments will be able to measure this parameter even if it is at the minimum of its allowed range.

- Inflation predicts that density perturbations are:
 - approximately scale-invariant (parameterized by n_s).
 - approximately Gaussian.
- The CMB is currently the primary means to test these predictions and it confirms $n_s \approx 0.96$ and non-Gaussian contributions are strongly constrained.
- Theoretically, inflation still remains as a paradigm. We do not know what kind of fields are responsible for the inflation.
- Single scalar field slow-roll inflation predicts negligible amounts of non-Gaussianity $f_{\text{NL}} \sim \mathcal{O}(0.01)$. Reference: Maldacena (2003), Creminelli & Zaldarriaga (2004).
- It seems unlikely that we can disentangle all these contaminations and detect such small primordial non-Gaussianities in the near future.
- So measuring non-Gaussianity $> \mathcal{O}(1)$ rules out single field inflation.

Planck and non-Gaussianity



Ade et al. (2015)

Current constraints

$$f_{\text{NL}} = 0.8 \pm 5.0$$

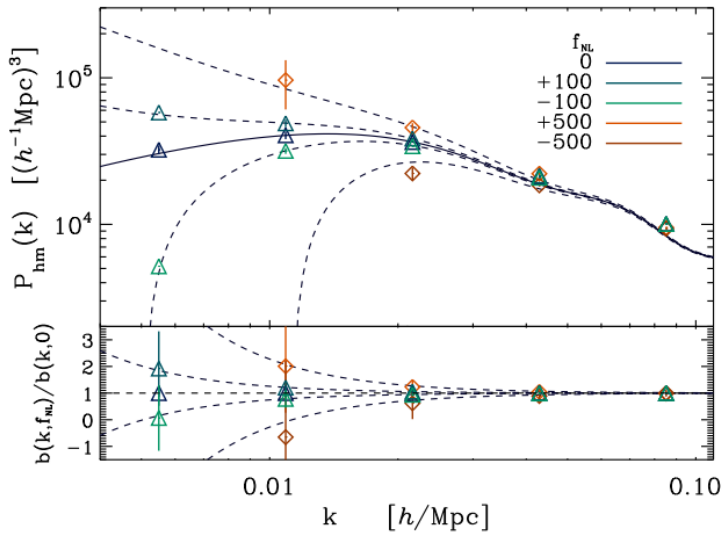
$$g_{\text{NL}} = -4 \pm 43$$

$$\tau_{\text{NL}} = -26 \pm 21$$

- Planck saturated the information on non-Gaussianity from temperature anisotropies... polarization might yield another factor of ~ 2 (foreground?).
- It will be very hard to do better than Planck with LSS (many possible sources of systematics, bispectrum seems very difficult).

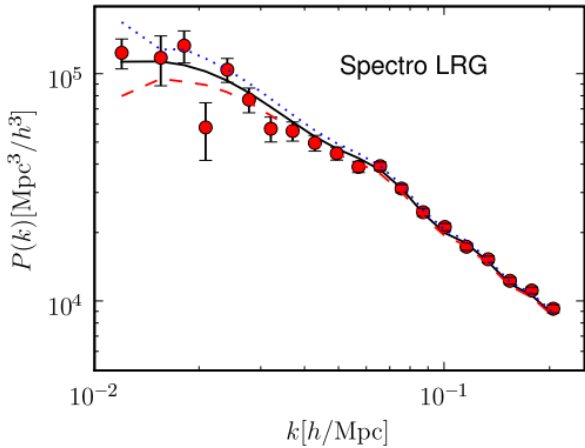
- Without primordial non-Gaussianity we can smooth a density field at the scale of gravitational non-Gaussianity and have a Gaussian density field. In that density field we would only have a linear bias.
- Primordial non-Gaussianity changes the clustering on large scales and makes the relation between halos and the density field scale-dependent $\propto f_{NL}(b - 1)k^{-2}$, Dalal et al. (2007). Such a scaling is hard to produce with local post inflation processes... and therefore represents a powerful cosmological test!
- Intuitively this works through correlations of small and large scale modes. In the Gaussian case, long and small scale modes are not correlated. With primordial non-Gaussianity they become correlated, meaning that in a peak of a large scale mode we get more haloes than expected and in a trough we get less.
- It has been shown that because of the large number of modes available in LSS, such constraints ultimately can be better than the constraints from the CMB.

LSS and non-Gaussianity



Dalal et al. (2007)

LSS and non-Gaussianity

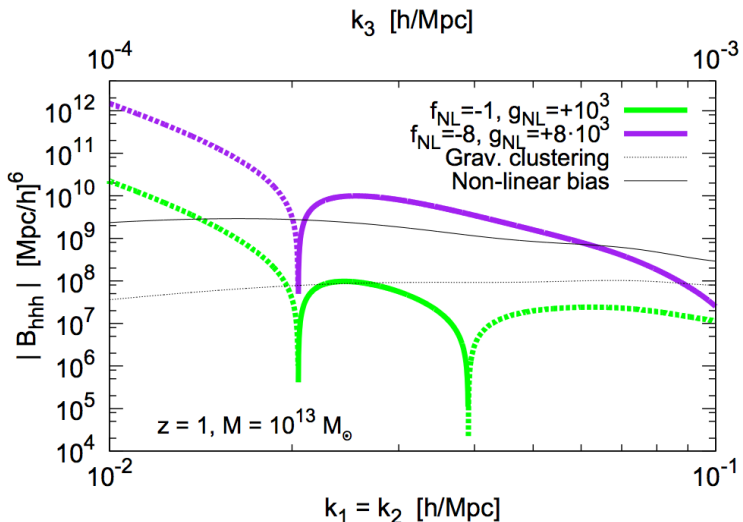


Slosar et al. (2008)

$$-29 < f_{\text{NL}} < 70 \quad (95\% \text{ CL})$$

- Using only the power spectrum does not allow to distinguish between different non-Gaussianity types. In the two-point function f_{NL} and g_{NL} are degenerate. These degeneracies can be broken by higher order statistics, Tasinato et al. (2014).
- While f_{NL} is usually used to describe local non-Gaussianity (skewness), g_{NL} is used in terms of the four point function (kurtosis)

LSS and non-Gaussianity



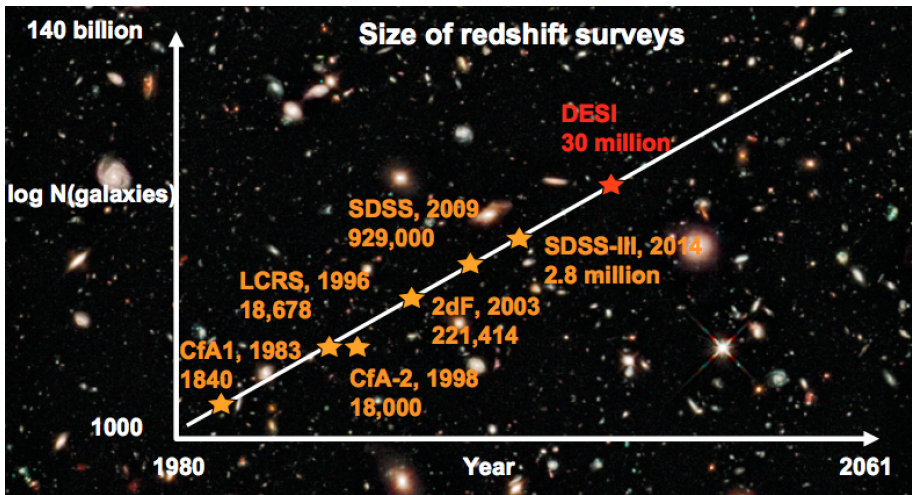
Tasinato et al. (2014)

- The CMB currently provides the best bounds on primordial non-Gaussianity and is consistent with the Gaussian case.
- Detection if primordial non-Gaussianity $> \mathcal{O}(1)$ could rule out single field inflation... non-detection can limit the parameter space for multi-field inflation models.
- Large scale structure observations should eventually overpower the CMB as a probe of fundamental physics (3D is better than 2D!).
- The current observational focus is on measuring the expansion history and growth of perturbations using clustering (BAO, RSD, ...) and lensing
- The fact that LSS is highly non-Gaussian is a blessing and a curse; it's an opportunity to think creatively about new cosmological observables.

Future outlook, DESI and Euclid

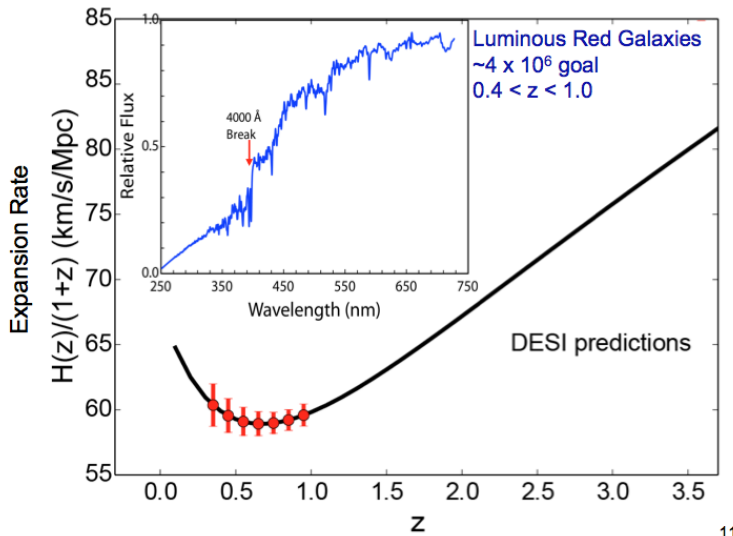
The Mayall 4m telescope on Kitt peak in Arizona, timescale 2018-2022



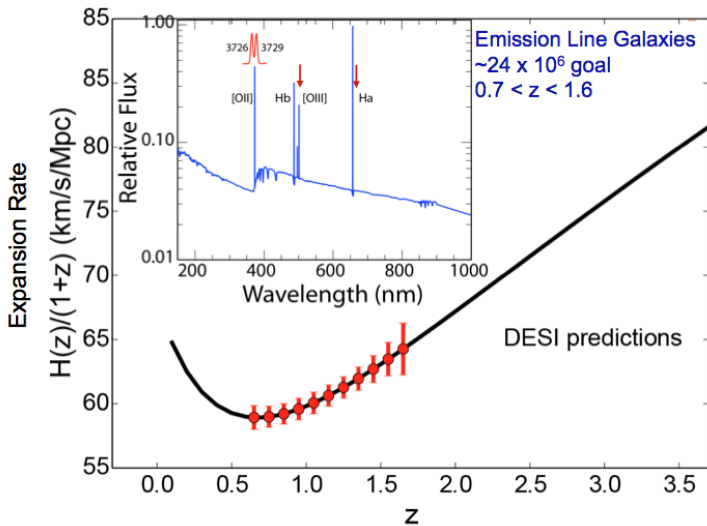


- An imaging (targeting) survey over 14 000 deg².
 - g-band to 24.0 mag
 - r-band to 23.6 mag
 - z-band to 23.0 mag
- A spectroscopic survey over 14 000 deg².
 - 4 million Luminous Red Galaxies
 - 23 million Emission Line Galaxies
 - 1.4 million quasars
 - 0.6 million quasars at $z > 2.2$ for Lyman-alpha-forest
- Covering a volume of $50h^{-3}\text{Gpc}^3$, compared to $6h^{-3}\text{Gpc}^3$ in BOSS.
- 5000 fibres compared to 1500 fibres in BOSS (automatic fibre positioner).

Future outlook, DESI and Euclid

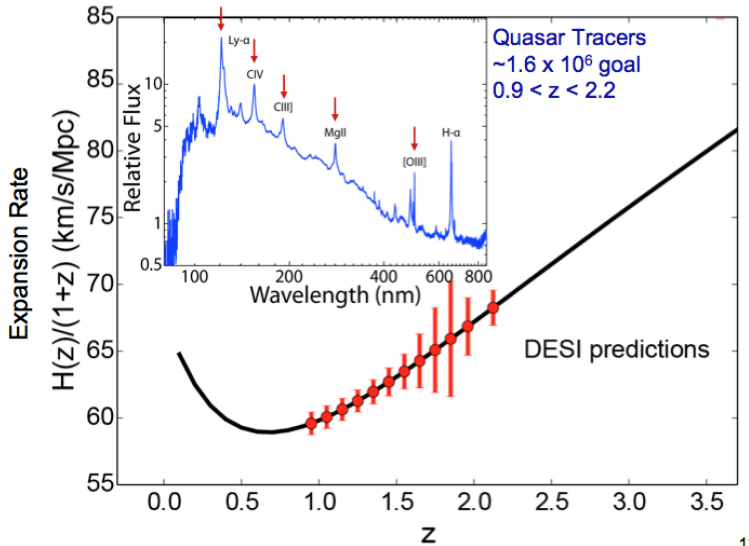


Future outlook, DESI and Euclid



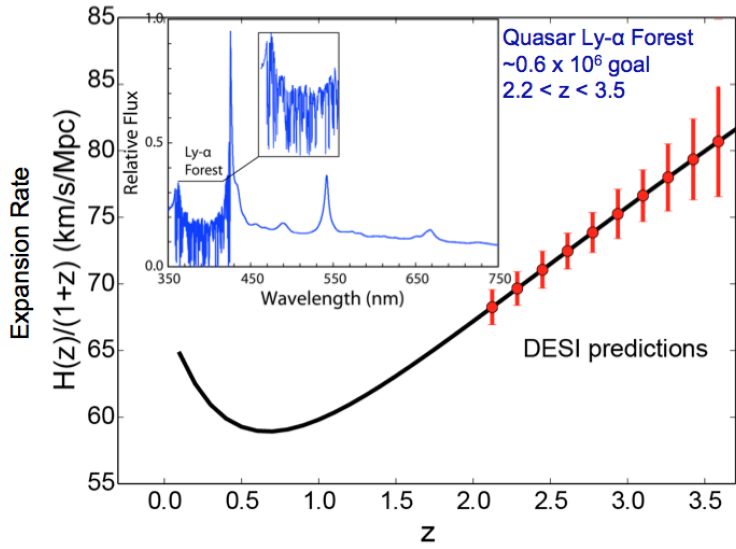
12

Future outlook, DESI and Euclid

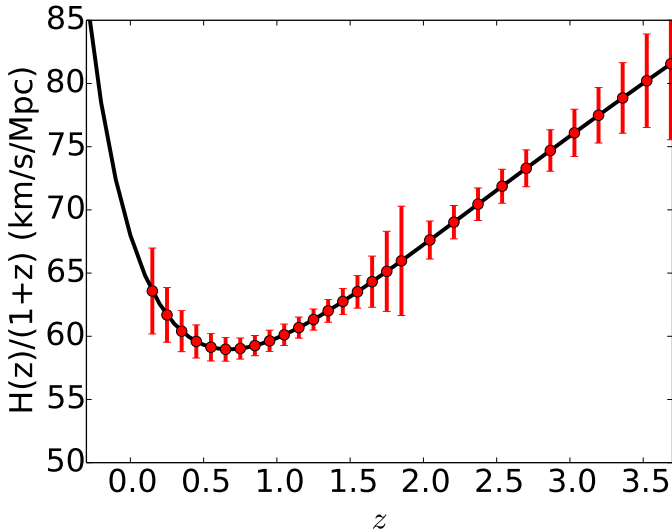


1:

Future outlook, DESI and Euclid

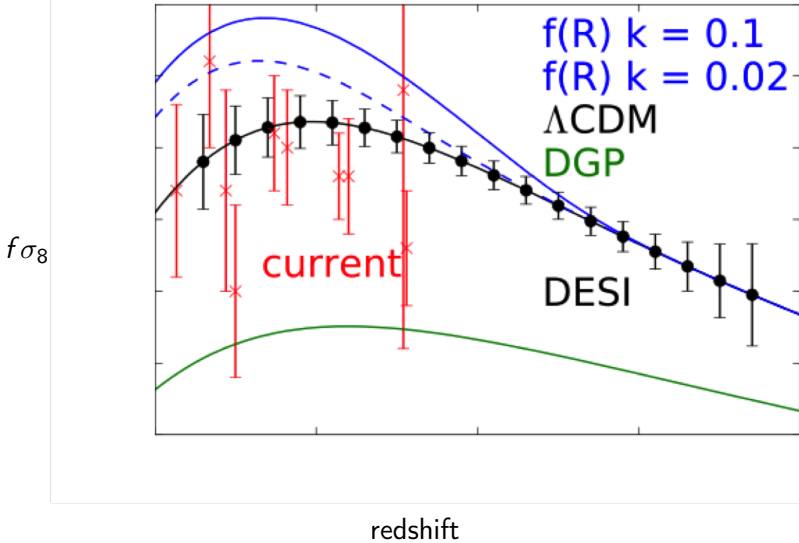


Future outlook, DESI and Euclid



credit: Patrick McDonald

Future outlook, DESI and Euclid

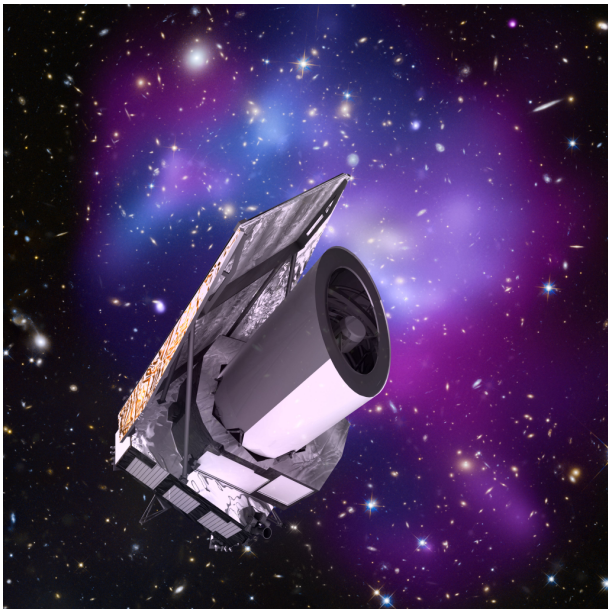


Main science goals are:

- Distance-redshift relation:
 - Measure distance scale to $< 0.3\%$ between $0.0 < z < 1.1$.
 - Measure distance scale to $< 0.3\%$ between $1.1 < z < 1.9$.
 - Measure the Hubble parameter to $< 1\%$ in the bin $1.9 < z < 3.7$.
- Constrain the growth factor at \sim a few percent level up to $z=1.5$
- Beyond Dark Energy:
 - Constrain spectral index of primordial perturbations and its running to $< 0.4\%$
 - Measure the neutrino masses to $< 0.017 \text{ eV}$

Reference: Font-Ribera et al. (2014)

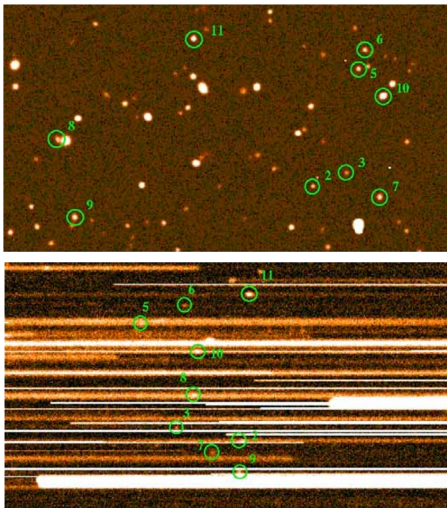
Future outlook, DESI and Euclid



The Euclid mission

- Euclid is a 5 year ESA space mission to observe $15\,000 \text{ deg}^2$.
- 1.2m mirror connected to an imager and slitless spectrograph (redshift detection through the $\text{H}\alpha$ line).
- Visible and near-infrared imaging and near-infrared spectroscopy.
- ~ 10 billion photometric sources and ~ 10 millions spectroscopic redshifts.
- Main science motivation is galaxy clustering and weak lensing.
- Slitless spectroscopy works best in sparsely populated fields, as it spreads each point source out into its spectrum, and crowded fields will have to deal with source confusion.

Future outlook, DESI and Euclid



Future outlook, DESI and Euclid



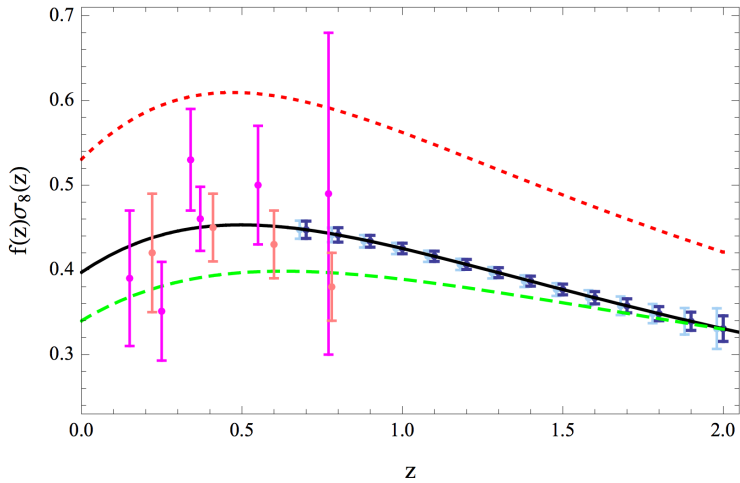
- Euclid images of $z \sim 1$ galaxies: same resolution as SDSS images at $z \sim 0.05$ and at least 3 magnitudes deeper.
- Space imaging of Euclid will outperform any other weak lensing survey.

Future outlook, DESI and Euclid

Euclid science case

Parameter	Modified Gravity	Dark Matter	Initial Conditions	Dark Energy		
	γ	m_ν/eV	f_{NL}	w_p	w_a	FoM
Euclid Primary	0.010	0.027	5.5	0.015	0.150	430
Euclid All	0.009	0.020	2.0	0.013	0.048	1540
Euclid+Planck	0.007	0.019	2.0	0.007	0.035	4020
Current	0.200	0.580	100	0.100	1.500	\sim 10
Improvement Factor	30	30	50	>10	>50	>300

Future outlook, DESI and Euclid



Majerotto et al. (2012)

Thank you very much